

FLORIDA INTERNATIONAL UNIVERSITY

Miami, Florida

EXPERIMENTAL INVESTIGATION OF WIND-INDUCED
RESPONSE OF SPAN-WIRE TRAFFIC SIGNAL SYSTEMS

A thesis submitted in fulfillment of
the requirements for the degree of

MASTER OF SCIENCE

in

CIVIL ENGINEERING

by

Manuel A. Matus

2018

To: Dean John Volakis
College of Engineering and Computing

This dissertation, written by Manuel A. Matus, and entitled Experimental Investigation of Wind-induced Response of Span-wire Traffic Signal Systems, having been approved in respect to style and intellectual content, is referred to you for judgment.

We have read this dissertation and recommend that it be approved.

Amal Elawady

Arindam Gan Chowdhury

Peter Irwin

Ioannis Zisis, Major Professor

Date of Defense: March 27, 2018

The dissertation of Manuel A. Matus is approved.

Dean John Volakis
College of Engineering and Computing

Andres G. Gill
Vice President for Research and Economic Development
And Dean of the University Graduate School

Florida International University, 2018

ACKNOWLEDGMENT

I would like to express my sincere gratitude to my Major Professor and supervisor Dr. Ioannis Zisis whose advice, suggestions and patient guidance throughout my time as his student has brought me to the conclusion of this thesis. I must say that I find myself lucky to have a supervisor like Dr. Ioannis Zisis as he showed care about my work and responded to my questions and queries promptly. His mentorship and lectures helped me acquire the knowledge to carry out research and develop my thesis. Also, I would like to acknowledge Dr. Arindam Gan Chowdhury, whose advice and lectures have enhanced my knowledge and understanding of this engineering field.

I would like to express my thanks to the Wall of Wind staff members, whose professionalism and vast experience in wind tunnel testing helped me tremendously with the experimental work. Completing this thesis would have been much more difficult without the help, support and friendship provided by my supervisor and staff of the Wall of Wind facility.

Finally, I would like to thank the financial support from Florida Department of Transportation. Most importantly, their advising, mentoring and guidance was a tremendous help during the entire process of this research project.

ABSTRACT OF THE THESIS

EXPERIMENTAL INVESTIGATION OF WIND-INDUCED RESPONSE OF SPAN-WIRE TRAFFIC SIGNAL SYSTEMS

by

Manuel A. Matus

Florida International University, 2018

Miami, Florida

Professor Ioannis Zisis, Major Professor

The purpose of this investigation was to identify key design parameters that might significantly affect the response of span wire traffic light systems during extreme wind events. The performance of these systems was assessed through physical testing in an effort to quantify the effect of sag ratio, wire tension and wire clearance. The Wall of Wind experimental facility at Florida International University was utilized for testing the systems at different wind speeds and wind directions.

The findings showed that, at all tested wind directions, lift, drag and tension forces increased with increasing wind speeds. On the contrary, increasing the wind speed resulted in higher inclination on the traffic lights, lower drag coefficients and higher lift coefficients. Overall, when the wind was approaching from the rear face of the traffic signals, increased drag coefficients were recorded. When the sag was set at 7% lower drag coefficients were observed.

TABLE OF CONTENT

CHAPTER	PAGE
1. Introduction	1
2. Experimental Methodology	3
2.1 Experimental Facility	3
2.2 Test Setup and Method.....	3
2.3 Instrumentation	15
2.4 Data Analysis	17
3. Results and Discussion	20
3.1 Wind Induced Forces	20
3.2 RMS of Accelerations	32
3.3 Inclinations of the Traffic Signals.....	34
3.4 Drag Coefficients	38
3.5 Lift Coefficients	42
4. Conclusion	45
References	47
Appendix.....	49

LIST OF TABLES

TABLE	PAGE
Table 1-1 - Traffic signal statistics for 2004 (FDOT 2005)	2
Table 2-1 - diagrams for wind angles of attack.....	7

LIST OF FIGURES

FIGURE	PAGE
Figure 2-1 - Testing facility flow management system and turn table diagram (Chowdhury et al., 2016).....	4
Figure 2-2 - Test rig with traffic light assembly mounted on turn table	4
Figure 2-3 - Direction of x, y, z components for each load cell (direction of each axis shown represents 'positive direction') (drawn by B. Berlanga 2015 modified by M. Matus).....	8
Figure 2-4 - Plan view of test rig (drawn by B. Berlanga 2015 modified by M. Matus)	9
Figure 2-5 – Profile elevation view of test rig (drawn by B. Berlanga 2015 modified by M. Matus).....	9
Figure 2-6 - End elevation view of test rig (drawn by B. Berlanga 2015 modified by M. Matus).....	10
Figure 2-7 - Test rig with traffic lights assembly	10
Figure 2-8 - Test rig set up.....	11
Figure 2-9 – Standard traffic light assembly (5% sag, 7 feet distance between catenary and messenger load cell, standard messenger wire pre-tension)	11
Figure 2-10 – Modified traffic light assembly (7% sag, 7 feet distance between catenary and messenger load cell, standard messenger wire pre-tension)	12
Figure 2-11 - Modified traffic light assembly (3% sag, 7 feet distance between catenary and messenger load cell, standard messenger wire pre-tension)	12
Figure 2-12 – Modified traffic light assembly (5% sag, 7 feet distance between catenary and messenger load cell, 75% of standard messenger wire pre-tension)	13
Figure 2-13 – Modified traffic light assembly (5% sag, 7 feet distance between catenary and messenger load cell, 125% of standard messenger wire pre-tension)	13
Figure 2-14 - Modified traffic light assembly (5% sag, 6.5 feet distance between catenary and messenger load cell, standard messenger wire pre-tension)	14
Figure 2-15 – Modified traffic light assembly (5% sag, 6 feet distance between catenary and messenger load cell, standard messenger wire pre-tension)	14
Figure 2-16 – Modified traffic light assembly (5% sag, 7 feet distance between	

catenary and messenger load cell, un-tensioned messenger wire)	15
Figure 2-17 - 6 degree of freedom load cell	16
Figure 2-18 - Location of accelerometers and inclinometers in 5-section signal	17
Figure 2-19 - Location of accelerometers and inclinometers in east 3-section signal ...	17
Figure 3-1 - Mean messenger wire drag forces	22
Figure 3-2 - Mean messenger wire tension forces	22
Figure 3-3 - Mean messenger wire lift forces	23
Figure 3-4 - Mean catenary wire drag forces	23
Figure 3-5 - Mean catenary wire tension forces	23
Figure 3-6 - Mean catenary wire lift forces	24
Figure 3-7 - Maximum & minimum messenger wire drag forces	26
Figure 3-8 - Maximum & minimum messenger wire tension forces	27
Figure 3-9 - Maximum & minimum messenger lift forces	28
Figure 3-10 - Maximum & minimum catenary drag forces	29
Figure 3-11 - Maximum & minimum catenary tension forces	30
Figure 3-12 - Maximum & minimum catenary lift forces	31
Figure 3-13 - Maximum vs mean messenger tension forces	31
Figure 3-14 - 5-section signal RMS of accelerations	33
Figure 3-15 - 3-section signal RMS of accelerations	34
Figure 3-16 - Mean along wind inclinations (Inc 7 and 8 at 5-section signal & Inc 5 and 6 at 3-section signal)	36
Figure 3-17 - Mean across wind inclinations (Inc 7 and 8 at 5-section signal & Inc 5 and 6 at 3-section signal)	37
Figure 3-18 – 5-section signal maximum inclinations along wind	37
Figure 3-19 – 3-section signal maximum inclinations along wind	38

Figure 3-20 - Drag coefficients vs wind speed.....	41
Figure 3-21 - Mean inclinations of traffic signals vs drag coefficients with standard deviation at 0 degrees wind angle of attack	41
Figure 3-22 - Mean inclinations of traffic signals vs drag coefficients with standard deviation at 180 degrees wind angle of attack.....	42
Figure 3-23 - Lift coefficients vs wind speed.....	44

APPENDIX

FIGURE.....	PAGE
A: 1 - mean lift forces 45 degrees	49
A: 2 - mean drag forces 45 degrees	50
A: 3 - mean tension forces 45 degrees.....	51
A: 4 - 3-section signal mean inclinations along wind 45 degrees.....	51
A: 5 - 5-section signal mean inclinations along wind 45 degrees.....	52
A: 6 - 3-section signal rms of accelerations 45 degrees	52
A: 7 - 5-section signal rms of accelerations 45 degrees	53
A: 8 - drag coefficients 45 degrees.....	53
A: 9 - lift coefficients 45 degrees	54
A: 10 - mean lift forces 135 degrees	55
A: 11 - mean drag forces 135 degrees	56
A: 12 - mean tension forces 45 degrees.....	57
A: 13 - 3-section signal mean inclinations along wind 135 degrees.....	57
A: 14 - 5-section signal mean inclinations along wind 135 degrees.....	58
A: 15 - 3-section signal rms of accelerations 135 degrees	58
A: 16 - 5-section signal rms of accelerations 135 degrees	59
A: 17 - drag coefficients 135 degrees.....	59
A: 18 - lift coefficients 135 degrees	60
A: 19 - mean lift forces 180 degrees	61
A: 20 - mean drag forces 180 degrees	62
A: 21 - mean tension forces 45 degrees.....	63

A: 22 - 3-section signal mean inclinations along wind 180 degrees.....	63
A: 23 - 5-section signal mean inclinations along wind 180 degrees.....	64
A: 24 - 3-section signal rms of accelerations 180 degrees	64
A: 25 - 5-section signal rms of accelerations 180 degrees	65
A: 26 - drag coefficients 180 degrees.....	65
A: 27 - lift coefficients 180 degrees	66

ABBREVIATIONS AND ACRONYMS

A	Area
ABL	Atmospheric Boundary Layer
Accel	Accelerometer
C_D	Drag Coefficient
C_L	Lift Coefficient
FDOT	Florida Department of Transportation
F_D	Drag Force
FIU	Florida International University
F_L	Lift Force (in formula)
F_x	Lift Force (in load cells)
F_y	Drag Force (in load cells)
F_z	Tension Forces
HSS	Hollow Structural Section
Inc	Inclinations/Inclinometer
Lbs	Pounds Force
LC	Load Cell(s)
MPH	Miles per Hour
RMS	Root Mean Square
V	Velocity
WOW	Wall of Wind
ϕ	Diameter
ρ	Density of Air

1. Introduction

Due to its geographic location, the state of Florida is prone to extreme wind events, such as hurricanes. These extreme events can cause significant damage to civil engineering infrastructure systems, including traffic signals. Wind-induced damages to traffic signals can greatly affect traffic flow within a city as well evacuation during or after major wind events. Although mast arm intersections are preferred, span-wire intersections are still the most common intersection found in South Florida and are still used when a mast arm intersection cannot be installed due to physical constraints. According to Florida Department of Transportation (FDOT), and as shown in Table 1-1, there were 9667 intersections using span-wire systems and 5643 intersections using mast arms district wide. Although the wide usage of span-wire traffic light systems at intersections, there is limited information available in the literature on the safe design of such systems under wind forces (Cook et al., 2012, Zisis et al., 2016). In fact, the performance of vehicular traffic signals during the 2004-2005 hurricane season indicated that these systems need to be carefully studied to assess their performance and achieve a better design (Cook et al., 2012). Enhancing their survivability during and after extreme wind events is important to the safety of motorists as the time to recover damaged traffic lights may be long and potentially impose a life threat (Sivarao et al., 2010).

Table 1-1 - Traffic Signal Statistics for 2004 (FDOT 2005)

District	Total Np. Of Signals District-wide*	Total Signals on the State Highway System	Total Signals on Local Roads	Total Mast Arm Signals District-wide*	Total Mast Arm Signals on the State Highway System	Total Span Wire Signals District wide*	Total Span Wire Signals on the State Highway System
1	1778	981	797	802	432	976	542
2	1585	1125	460	537	437	1048	688
3	987	687	300	300	280	687	407
4	3329	1778	1551	1180	1062	2149	1165
5	2972	1479	1493	458	325	2514	1154
6	2640	1341	1299	1848	938	660	403
7	2151	1018	1133	518	263	1633	755
Turnpike	None			None			
Total	15442	8409	7033	5643	3737	9667	5114

2. Experimental Methodology

2.1 Experimental Facility

The experimental work of this research was carried out at the Wall of Wind (WOW) experimental facility which is located at Florida International University (FIU), FL USA. This research facility has unique properties that allow for wind and rain testing of large and full-scale structures such as low-rise buildings, building components, infrastructure systems, bridges, etc. (Mooneghi et al., 2014, Kargarmoakhar et al., 2015, Chowdhury et al., 2016, Meyer et al., 2017). This facility is comprised of 12 fans of 700 horse power each that can reach up to 157 MPH wind speeds, that is category 5 hurricane wind forces in the Saffir-Simpson scale. The WOW has a flow management system that can be configured to simulate different types of the atmospheric boundary layer (ABL), as shown in Figure 2-1. For this investigation, the roughness elements of the flow management system were configured to produce an open terrain exposure (exposure C, ASCE 7-10). The WOW test section is equipped with a 16-foot-diameter turn table that can hold the test specimens in the wind path while allowing their rotation during the test (Figure 2-2).

2.2 Test Setup and Method

Due to the length of a typical span wire system found on the field, which may range from 50 to 130 feet long, a short span test rig with coil springs was utilized (Irwin et al., 2016). This short span rig possessed the same force to lateral deflection properties as a typical 80 feet long span found on the field. The benefit of utilizing this short span rig at the WOW is that it allows to test the assembly under different wind angles of attack, as the test rig is mounted on the turn table.

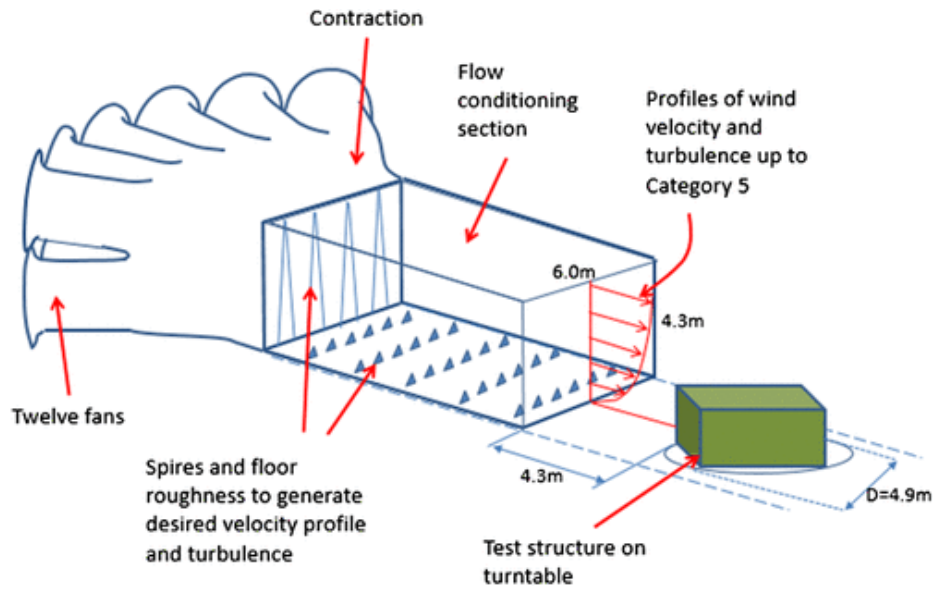


Figure 2-1 - Testing facility flow management system and turn table diagram (Chowdhury et al., 2016)

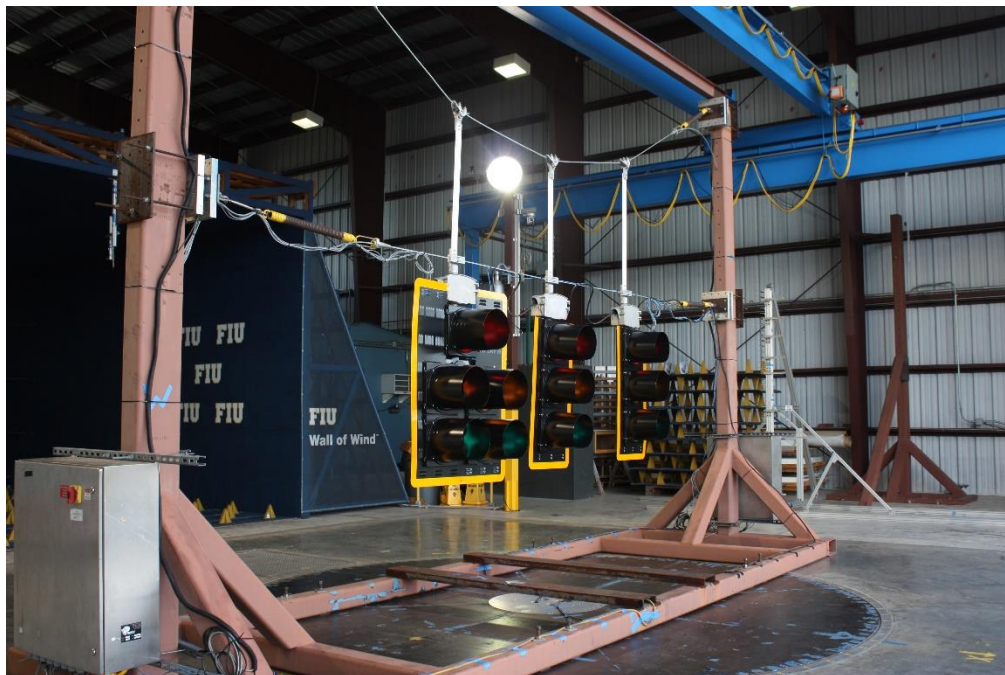


Figure 2-2 - Test rig with traffic light assembly mounted on turn table

The short span test rig was developed using the SAP2000 finite element structural analysis and design software and drafted on AutoCAD 2014 and modified with AutoCAD 2018. There were two different hollow structural sections (HSS) that were utilized, HSS 10" x 6" x 3/8" and HSS 6" x 6" x 3/8". The total length of the test rig is 21.9 feet and the width is 7.5 feet. The two support columns are 15.5 feet tall supported on top of HSS 10" x 6" x 3/8" sections and connected with an I section of 6" x 3 3/8", as shown in Figure 2-3. A plan view of the test rig is shown in Figure 2-4, a profile elevation view is shown in Figure 2-5, and an end elevation view is shown in Figure 2-6. A picture of the test rig with traffic signals is shown in Figure 2-7.

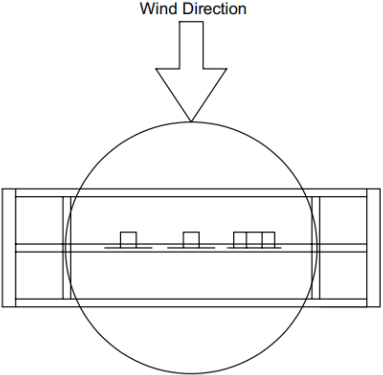
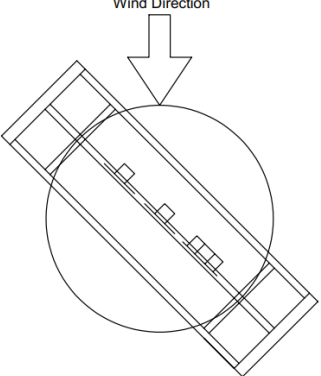
The installation requirements for span wire systems are specified in the FDOT Standard Specifications for Road and Bridge Construction, Section 634-3 (Standard Specifications for Road and Bridge Construction, 2017). The span wire assembly for this investigation was installed following FDOT standards to assess the performance of the system with default characteristics. To achieve the same force to deflection characteristics of a typical 80 feet long span wire system with a short test rig, coil springs were connected to an eyebolt that was welded to the top plate of the load cell which was attached to the test rig column, then a 3/8-inch diameter catenary and messenger wires were connected to the end of the coils and adjusted as per FDOT standards, as shown in Figure 2-8. The catenary cable was configured to represent 5% sag in the field, as per FDOT standards. Therefore, four times the sag ratio was required for the catenary wire used on the test rig to maintain the same lateral stiffness, which resulted in a sag length of 4 feet in the rig, for the 5% Sag FDOT standard installation.

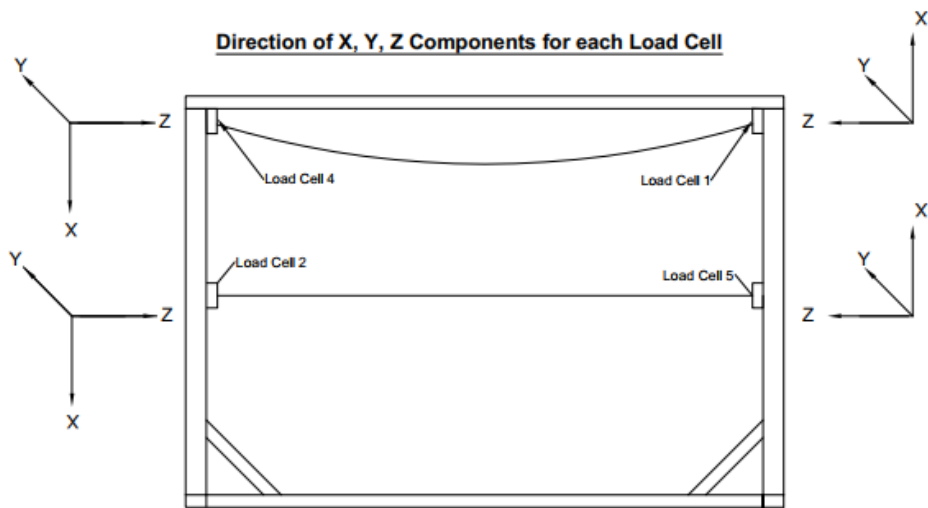
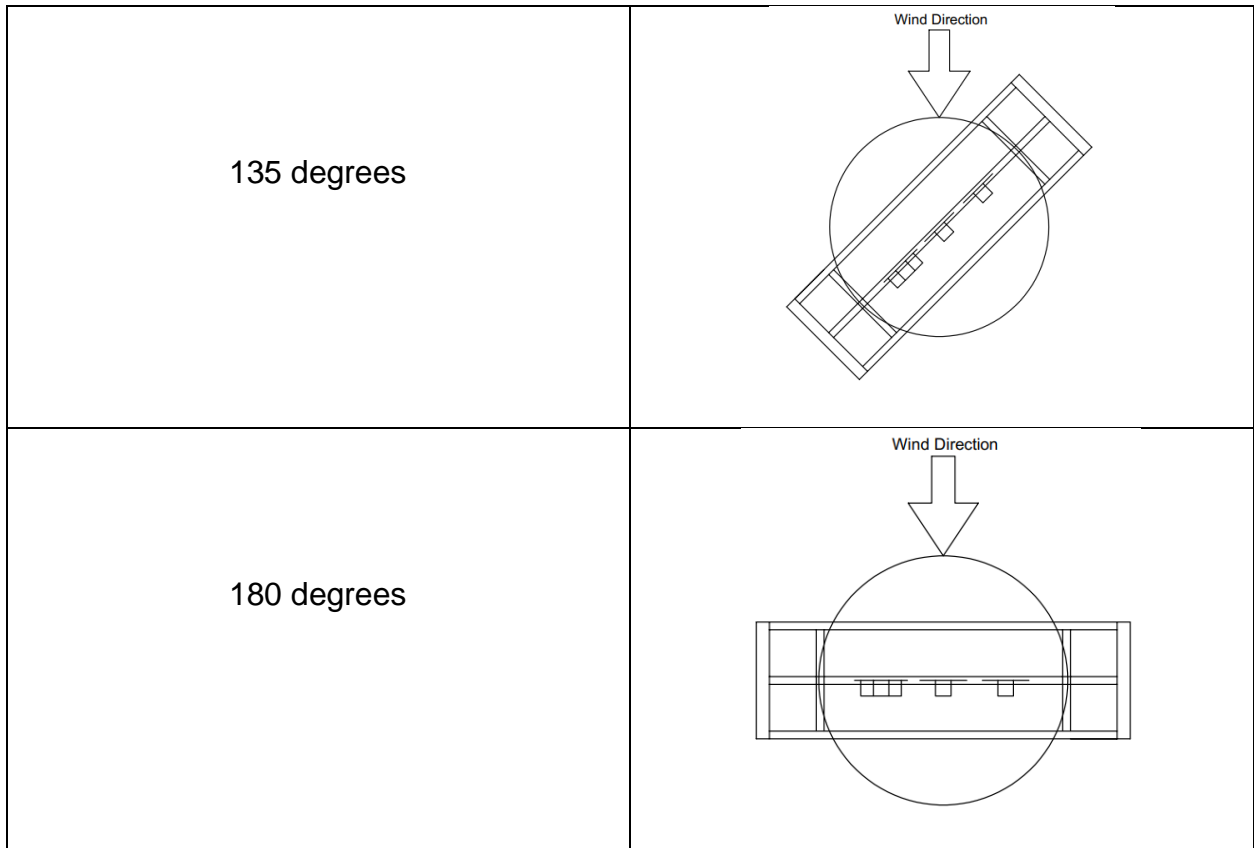
The center of the circular load cell at both ends of the messenger cable was located approximately 7 feet below the top catenary load cells. Due to the short span length, which is about $\frac{1}{4}$ of a typical span, the messenger cable tension was adjusted to approximately 80 lbs (i.e. per FDOT Standard Specifications for Road and Bridge Construction, Section 634-3, 3/8-inch wire diameter). The standard tension for a 3/8-inch diameter messenger wire is 340 lbs/100 feet, linearly prorating cable tensions for other lengths. Additional details about the short span test rig design are discussed in Irwin et al. (2016).

The test set up was first tested for 'no wind' conditions before every wind speed being tested and the values of the various data (forces, accelerations and inclinations) obtained were later deducted from the data obtained for different wind speeds (also known as "zero drift removal" process). The first test performed had all parameters as per FDOT standards; i.e. catenary wire sag (5%), catenary load cells location (7 feet above the messenger wire load cells) and messenger wire pre-tension of 80 lbs (Figure 2-9). After the first test was performed, one parameter of the traffic light assembly was changed at a time to assess the overall response of the system due to the corresponding modification. In the first modification the assembly was tested with a 7% sag, as shown in Figure 2-10. In the second modification the assembly was tested with a 3% Sag, as shown in Figure 2-11. The third modification assessed the performance of the traffic light assembly with 75% of the standard messenger wire pre-tension, as shown in Figure 2-12. In the fourth modification the messenger wire pre-tension was changed to 125% of the standard messenger wire pretension, as shown in Figure 2-13. In the fifth case the modified assembly was tested with a location of catenary load cells 6 inches below its original

location, as shown in Figure 2-14. In the sixth modification the traffic light assembly was tested with a location of catenary load cells 12 inches below its original location, as shown in Figure 2-15. The seventh modification assessed the performance of the assembly with an un-tensioned messenger wire, as shown in Figure 2-16. All cases were tested at 30, 45, 60 and 75 MPH wind speed and at angles of 0, 45, 135 and 180 degrees. Table 2-1 shows diagrams of each wind angle of attack.

Table 2-1 - Diagrams for wind angles of attack

Wind Angle of Attack	Diagram
0 degrees	
45 degrees	



Item:	Structural Traffic Signal Support
University:	Florida International University
Drawn by:	B. Berlanga
Updated by:	M. Matus
Date:	3/9/2018

Figure 2-3 - Direction of x, y, z components for each load cell (direction of each axis shown represents 'positive direction') (drawn by B. Berlanga 2015 modified by M. Matus)

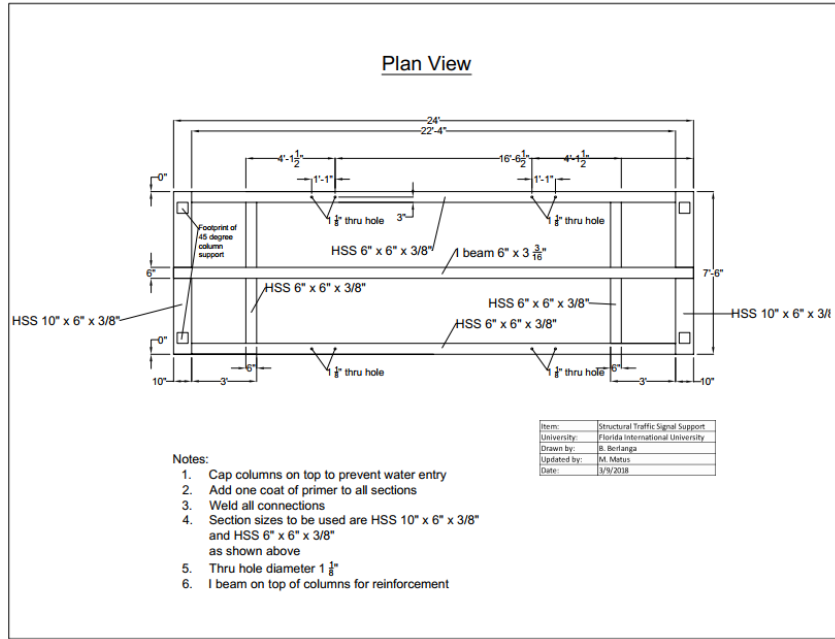


Figure 2-4 - Plan view of test rig (drawn by B. Berlanga 2015 modified by M. Matus)

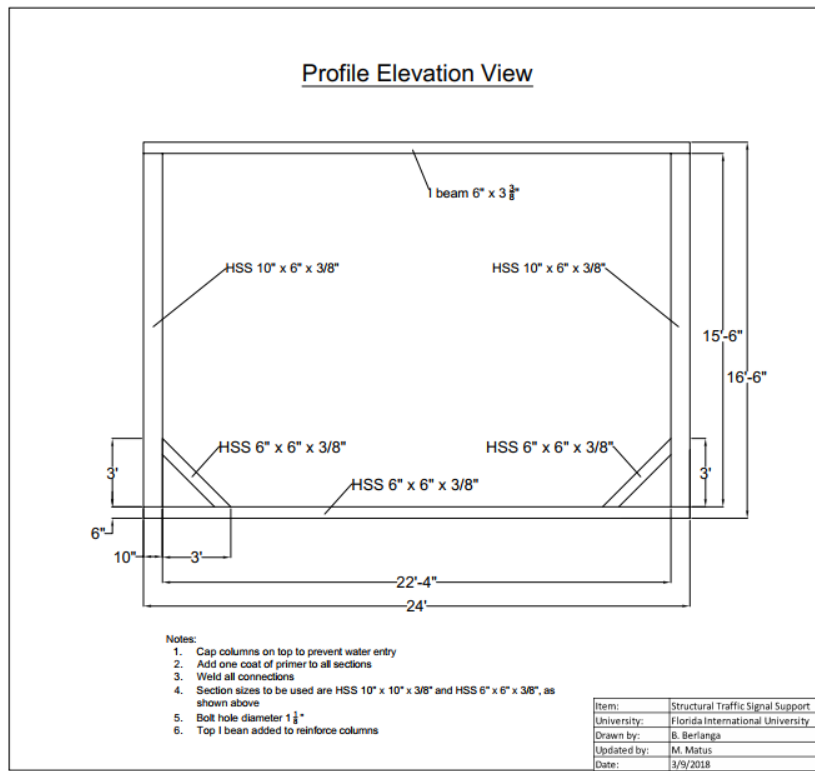


Figure 2-5 – Profile elevation view of test rig (drawn by B. Berlanga 2015 modified by M. Matus)

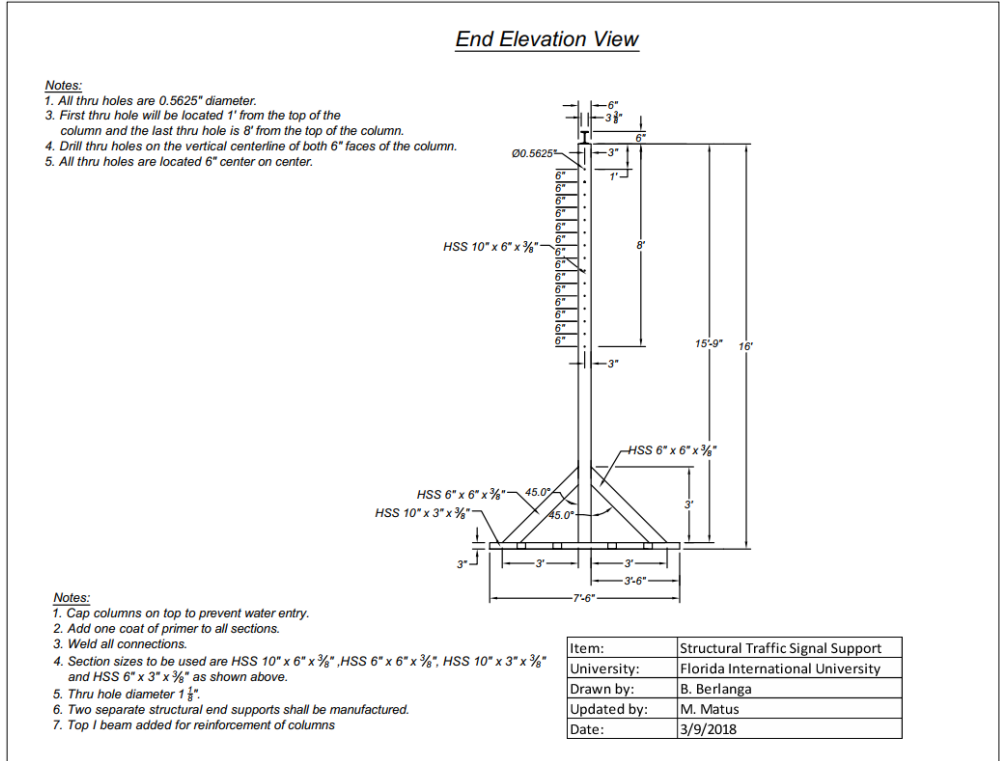


Figure 2-6 - End elevation view of test rig (drawn by B. Berlanga 2015 modified by M. Matus)



Figure 2-7 - Test rig with traffic lights assembly



Figure 2-8 - Test rig set up

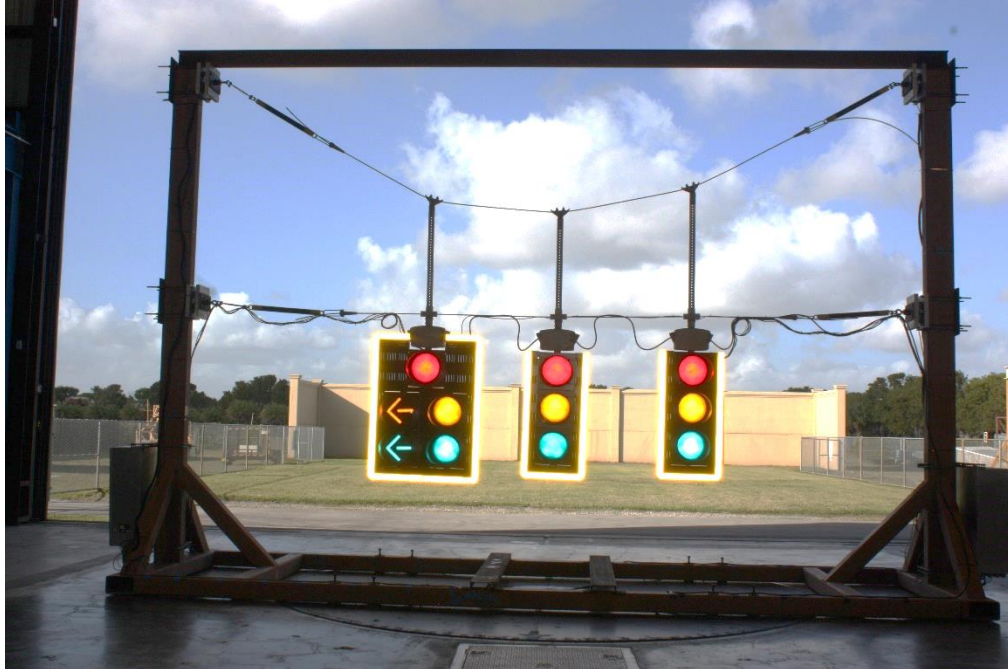


Figure 2-9 – Standard traffic light assembly (5% sag, 7 feet distance between catenary and messenger load cell, standard messenger wire pre-tension)

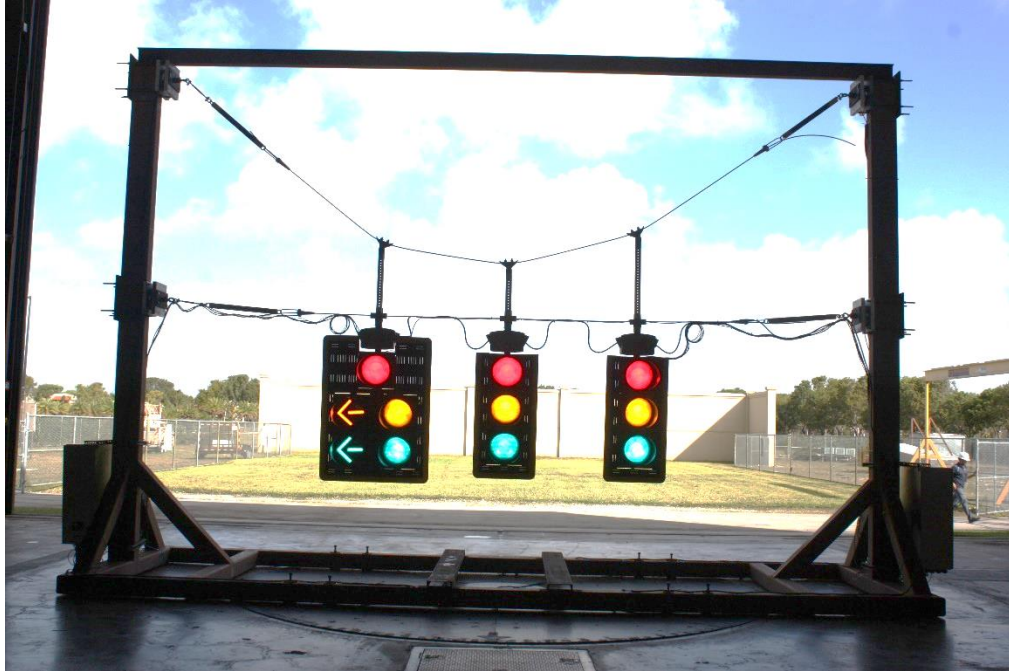


Figure 2-10 – Modified traffic light assembly (7% sag, 7 feet distance between catenary and messenger load cell, standard messenger wire pre-tension)



Figure 2-11 - Modified traffic light assembly (3% sag, 7 feet distance between catenary and messenger load cell, standard messenger wire pre-tension)

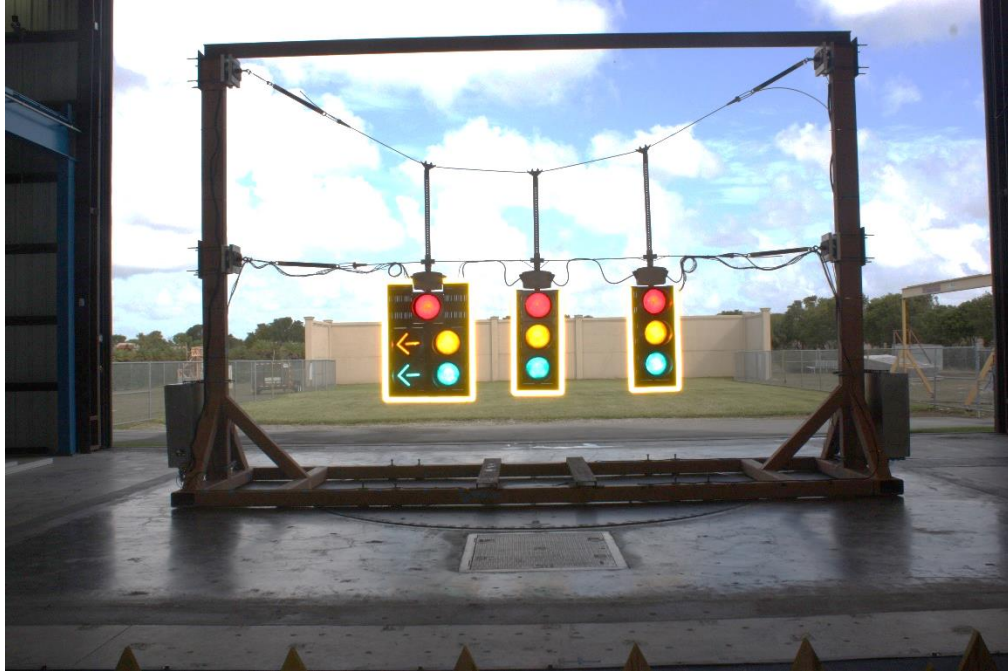


Figure 2-12 – Modified traffic light assembly (5% sag, 7 feet distance between catenary and messenger load cell, 75% of standard messenger wire pre-tension)



Figure 2-13 – Modified traffic light assembly (5% sag, 7 feet distance between catenary and messenger load cell, 125% of standard messenger wire pre-tension)



Figure 2-14 - Modified traffic light assembly (5% sag, 6.5 feet distance between catenary and messenger load cell, standard messenger wire pre-tension)

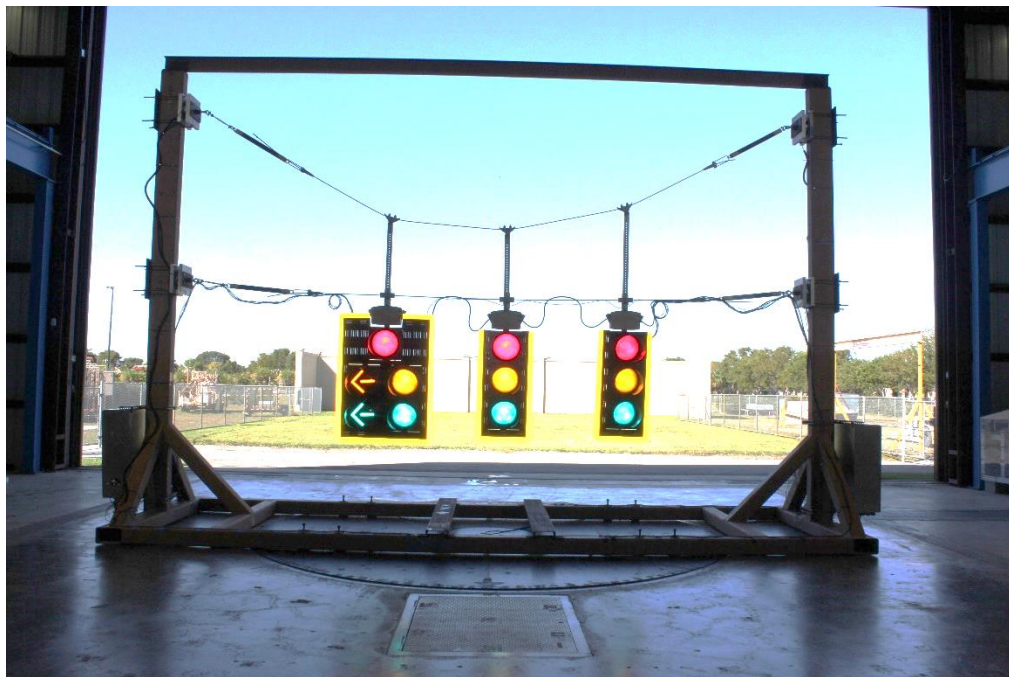


Figure 2-15 – Modified traffic light assembly (5% sag, 6 feet distance between catenary and messenger load cell, standard messenger wire pre-tension)



Figure 2-16 – Modified traffic light assembly (5% sag, 7 feet distance between catenary and messenger load cell, un-tensioned messenger wire)

2.3 Instrumentation

The instruments used during testing included four 6-degree of freedom load cells, six tri-axial accelerometers and four inclinometers. The four load cells measured x, y and z, force and moment components at the ends of the catenary and messenger wires. The directions of the x, y and z components for each load cell are shown in Figure 2-3. The load cells have a capacity of 1500 lbs. A picture of a 6-degree of freedom load cell is shown in Figure 2-17. Load cells number 2 and 5 were located at either end of the messenger cable and load cells number 1 and 4 were located at either end of the catenary cable.

The tri-axial accelerometers were installed in the traffic signals to measure accelerations at different locations. There was one accelerometer placed at the center

top of the signal (Accel5), another placed at the bottom right side (Accel002) and a third placed at the bottom left side (Accel003) for the 5-section signal as shown in Figure 2-18. Accelerometer Accel007, was installed on the top center, accelerometer Accel004, was installed on the bottom left side and accelerometer Accel006, was installed on the bottom right side of the 3-section signal as shown in Figure 2-19.

Inclinometers were also installed on each signal to measure the inclination of the signals during wind action. The inclinometers measured inclination in two directions, one relative to an axis parallel to the wind direction and another relative to an axis perpendicular to the wind direction. Two inclinometers were installed on the top center of the signal (Inc8) and another on the bottom center of the signal (Inc7), for the 5-section signal as shown in Figure 2-18. Inclinometer Inc6 was installed on the top center and inclinometer Inc5 was installed on the bottom center of the of the 3-section signal as shown Figure 2-19.



Figure 2-17 - 6 degree of freedom load cell

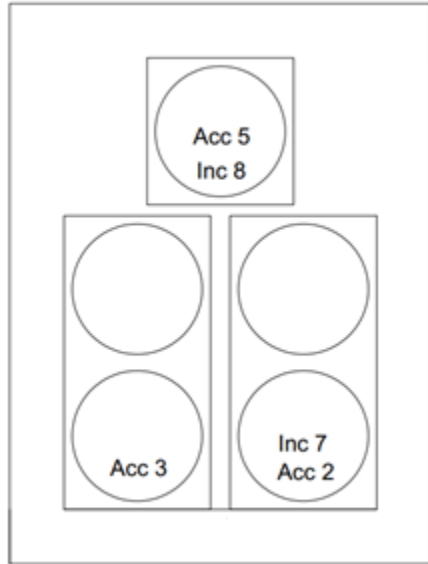


Figure 2-18 - Location of accelerometers and inclinometers in 5-section signal

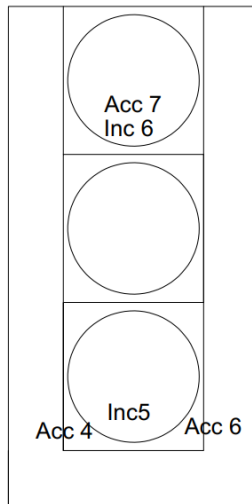


Figure 2-19 - Location of accelerometers and inclinometers in east 3-section signal

2.4 Data Analysis

To process the data, a “zero drift removal” process was performed to each case at every wind speed. For instance, at 0 degrees wind direction the following files were generated:

1. Baseline before 30mph test.
2. Data for 30 mph test.
3. Baseline before 45mph test.
4. Data for 45 mph test.
5. Baseline for 60 mph test.
6. Data for 60 mph test.
7. Baseline for 75 mph test.
8. Data for 75 mph test.

The mean for every component of the different instruments was calculated from the baselines and was subtracted from each data point of the data file that corresponds to that wind speed (i.e. time series data minus mean baseline). From this data, the mean, maximum and minimum value for each component of each instrument was calculated and reported. To find the RMS of accelerations, the standard deviation of the resultant acceleration of each accelerometer was taken.

For the drag and lift coefficients calculations, the total drag and lift forces were found by adding the 'y' components of all four load cells for drag and all 'x' components of all four load cells for lift forces. It needs to be noted that due to the orientation of the load cells, there were two load cells that had opposite orientation for the 'x' component, which had to be modified so that the four load cells measured positive values when pointing downward. For calculating the drag coefficients, the total frontal area of the span-wire system, the wind speed at the mean height of the traffic lights and the total drag force were used (see section 3.4). The total frontal area was found by adding one 5-section

plus two 3-section signals, coil springs, shackles and turnbuckles and the total frontal area was found to be about 30.7 ft². The wind speeds at the mean height of the traffic lights, which was about 64 inches from the floor, were calculated using the power law and the total drag force was the calculated summation of the 'Fy' of all four load cells. To calculate the lift coefficients, the same procedure utilized for the drag coefficient calculations was utilized, however, the total horizontal effective area was used instead, which attained a value of 10.3 ft², and the total lift force was used instead of the total drag force.

3. Results and Discussion

The results of this chapter are restricted to 0-degree wind direction. Additional wind direction results are presented in the appendix. Firstly, findings of mean and peak forces (in terms of lift forces, tension forces and drag forces) are discussed for all different tested cases, followed by the RMS of accelerations and the mean and maximum inclinations. The last section presents the analysis and interpretation of the findings in terms of drag and lift coefficients.

3.1 Wind Induced Forces

The directions of the forces of each load cell are shown in Figure 2-3. The mean and peak forces obtained at various wind speeds are discussed in this section. For all cases, the drag forces (F_y) on the messenger wire were found to increase as wind speed increased. At lower speeds, that is below 45 MPH, the drag forces of the messenger wire are similar and do not deviate noticeably from each other. However, when wind speed is higher than 45 MPH, the forces start to deviate from case to case. From all eight cases tested, the 3%-Sag case gave somewhat higher values of drag forces (F_y), while the 7%-Sag case gave the lowest drag forces (F_y) for both load cells 2 and 5 (Figure 3-1). The tension forces (F_z) of the messenger wire also increased as wind speed increased. The untensioned messenger case was the worst case and the 7%-Sag case the one with lower messenger wire tension forces, as shown in Figure 3-2. It should be noted that the different cases resulted in noticeable differences in mean tension forces even at lower wind speeds. The messenger wire lift forces (F_x) increased with increasing wind speed (Figure 3-3). As the convention of the weight and lift forces of the load cells is positive

downwards, an increase in the negative side of the curve indicates that the lift forces are increasing with increasing wind speeds. The lift force results indicate a relatively small absolute difference - about 10 lbs – between the various cases. Moreover, and in contrast to the previous results, the lift force values converge among the different cases at higher wind speeds.

The catenary wire drag forces (F_y) were found to be considerably lower than the messenger wire drag forces (Figure 3-4). As the wind speed was increased, some initial pre-tension was released and the trends started becoming negative. Moreover, the lights create a pivot point at the messenger wire and the catenary wire is pushed against the wind direction, thus going from positive to negative values. From all cases tested, it was found that the untensioned messenger case gave higher initial drag forces, which is justified, as the untensioned messenger wire does not produce a pivot at low wind speeds producing the whole span wire system to be displaced along wind. It is noteworthy that for some cases, and at about 60 MPH, the drag forces increased at a higher rate. The tension forces of the catenary wire are shown in Figure 3-5. All cases follow a negative slope trend with the negative sign of the forces to indicate the loss of the initial tension exerted on the catenary wire due to the weight of the traffic lights. As wind speed increased, lift forces increased therefore the tension of the catenary wire decreased. The graphs show the rate at which the tension forces decreased as wind made the lights to lift up. The 3%-sag case resulted in the worst absolute difference while the 7%-sag showed the least tension. As expected, the wind speed increase resulted in the increase of the lift forces (F_x) of the catenary wire (Figure 3-6). It needs to be noted that the same sign convention of the messenger wire load cells applies to the catenary load cells, being

upwards a positive convention, for the lift component. The findings indicate that there is not a considerable difference between the lift forces among the tested cases.

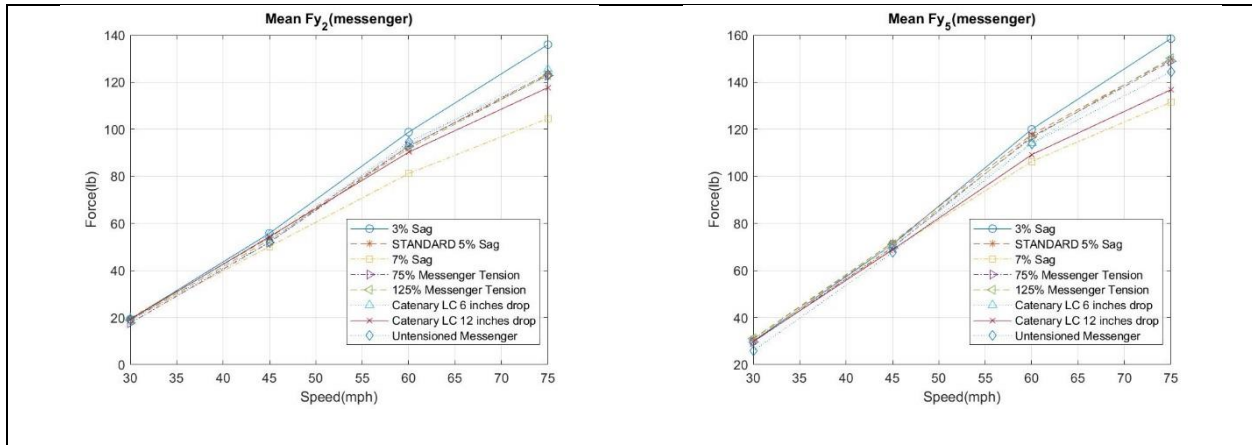


Figure 3-1 - Mean messenger wire drag forces

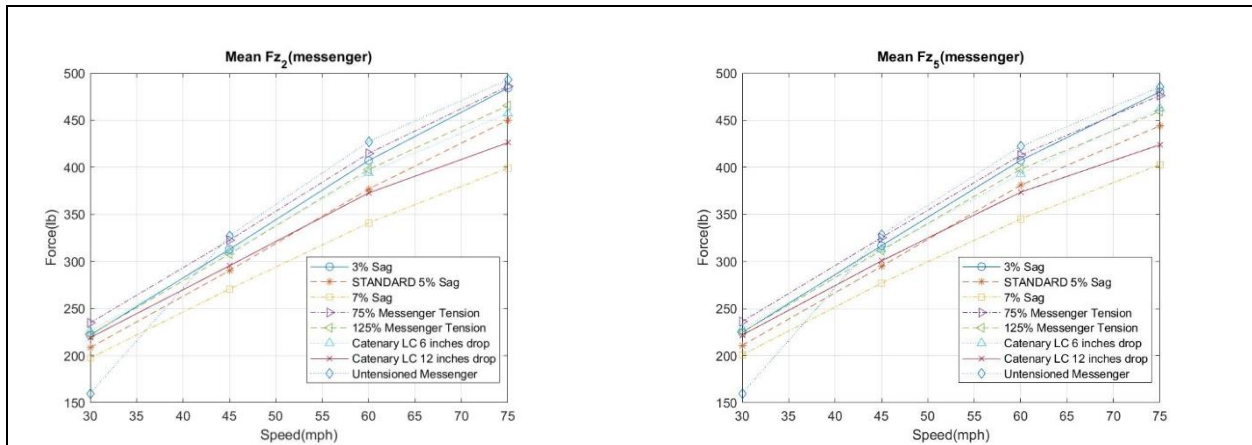


Figure 3-2 - Mean messenger wire tension forces

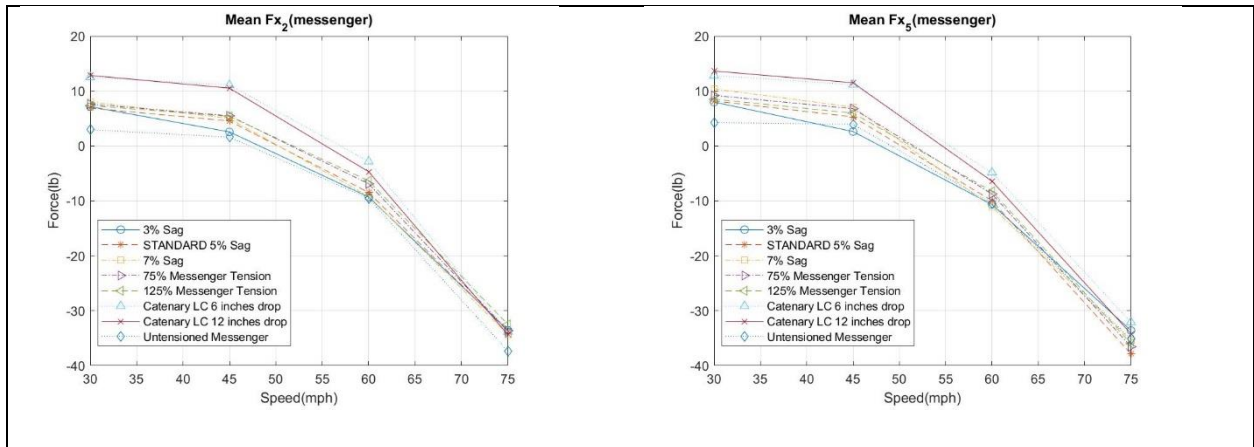


Figure 3-3 - Mean messenger wire lift forces

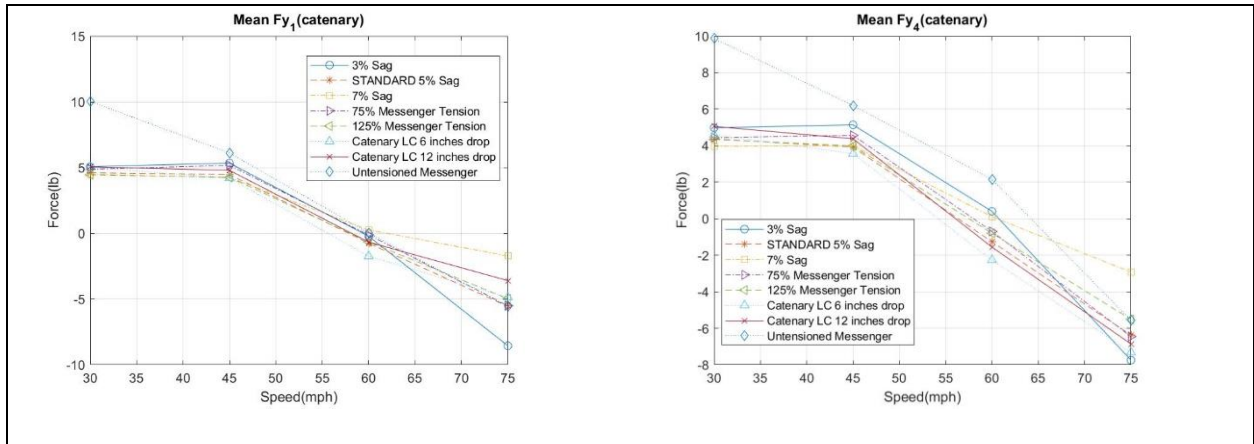


Figure 3-4 - Mean catenary wire drag forces

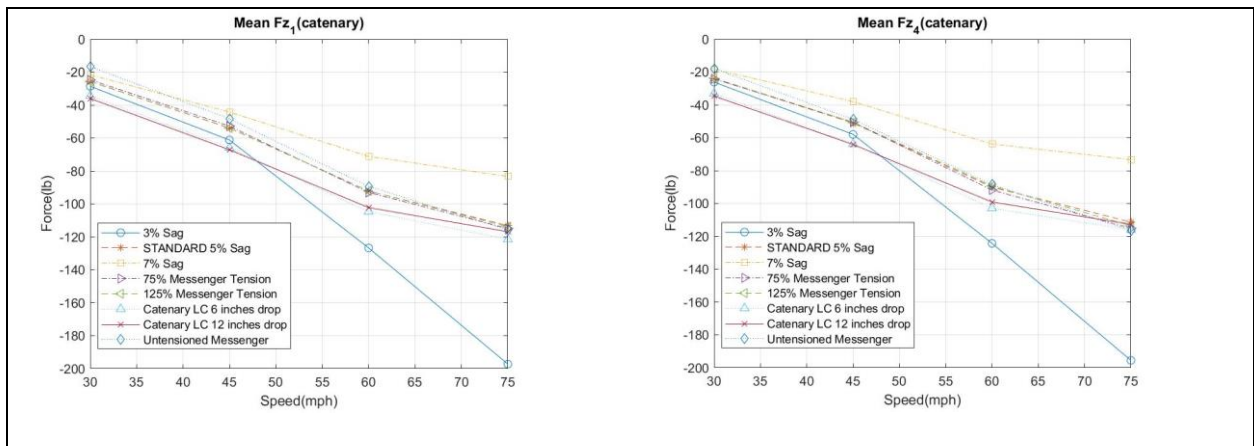


Figure 3-5 - Mean catenary wire tension forces

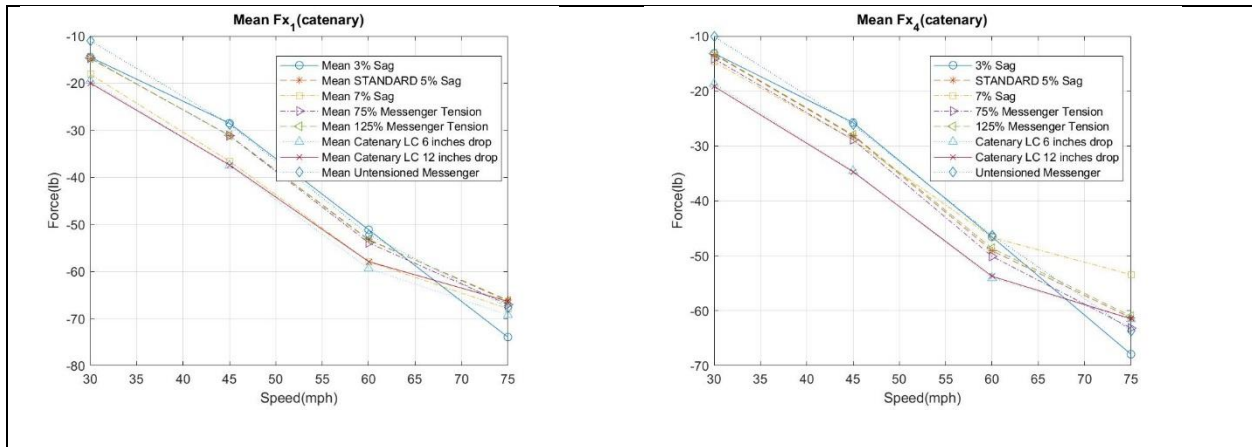


Figure 3-6 - Mean catenary wire lift forces

Similarly to the mean values, the maximum and minimum drag forces also increased with increasing wind speed (Figure 3-7). For the messenger wire forces, it was found that the worst maximum drag force was produced by the 3%-Sag case, attaining a value of about 178 lbs at 75 MPH while the lowest maximum drag force was produced by the 7%-Sag case, attaining a value of approximately 150 lbs at 75 MPH.

The maximum and minimum tension forces of the messenger wire were also found to increase as wind speed increased (Figure 3-8). The cases that were found to have experienced the highest tension forces of the messenger wire were the untensioned-messenger case, the 3%-Sag and the 75%-messenger-tension case, attaining a value of about 520 lbs. This shows that for these three modifications, an increase in the maximum tensions experienced by the messenger wire should be expected. The lowest maximum tension was found during the 7%-Sag case, which attained a value of about 450 lbs at 75 MPH (Figure 3-8).

For the lift forces, it was found that as wind speed is increased, the lift forces start to increase making the forces to go from a positive measurement (being the weight pointing

downwards) to a negative measurement. This means that as wind speed is increased, lights start pulling the cables up, thus giving measures of negative values after weight has been counteracted by the lift force. For the messenger wire, the critical minimum lift force was found to be about 49 lbs at 75 MPH in the untensioned-messenger case, as shown in Figure 3-9.

As explained previously, the catenary wire drag forces are of very small magnitudes and they increase in the positive range until a pivot point is formed at the messenger-wire to hanger connection. After that, the rate of change is negative; i.e. the lights produced some type of lever that pushed the catenary wire against the wind direction, resulting in negative numbers. The maximum drag force for the catenary wire was found to be about 18 lbs while the lowest catenary wire drag force was produced in the 7%-Sag case, as shown in Figure 3-10. Figure 3-11 shows the maximum and minimum rates at which the tension forces decreased, as previously explained. The lift forces showed an increase in magnitude as wind speed was increased and the maximum absolute value of lift force was found to be 90 lbs at 75 MPH with the 3%-Sag case, as shown in Figure 3-12. The least critical maximum absolute lift force experienced by the catenary wire was during the 7%-Sag case, attaining a value of 62 lbs at 75 MPH, as shown in Figure 3-12.

When comparing the mean forces to the maximum forces of the messenger tension forces, as seen in Figure 3-13, it can be seen that the maximum values are higher than the mean forces by about 50 lbs for all cases. At low speeds, the values are very similar and as wind speed is increased, the values between mean and maximum forces start to deviate.

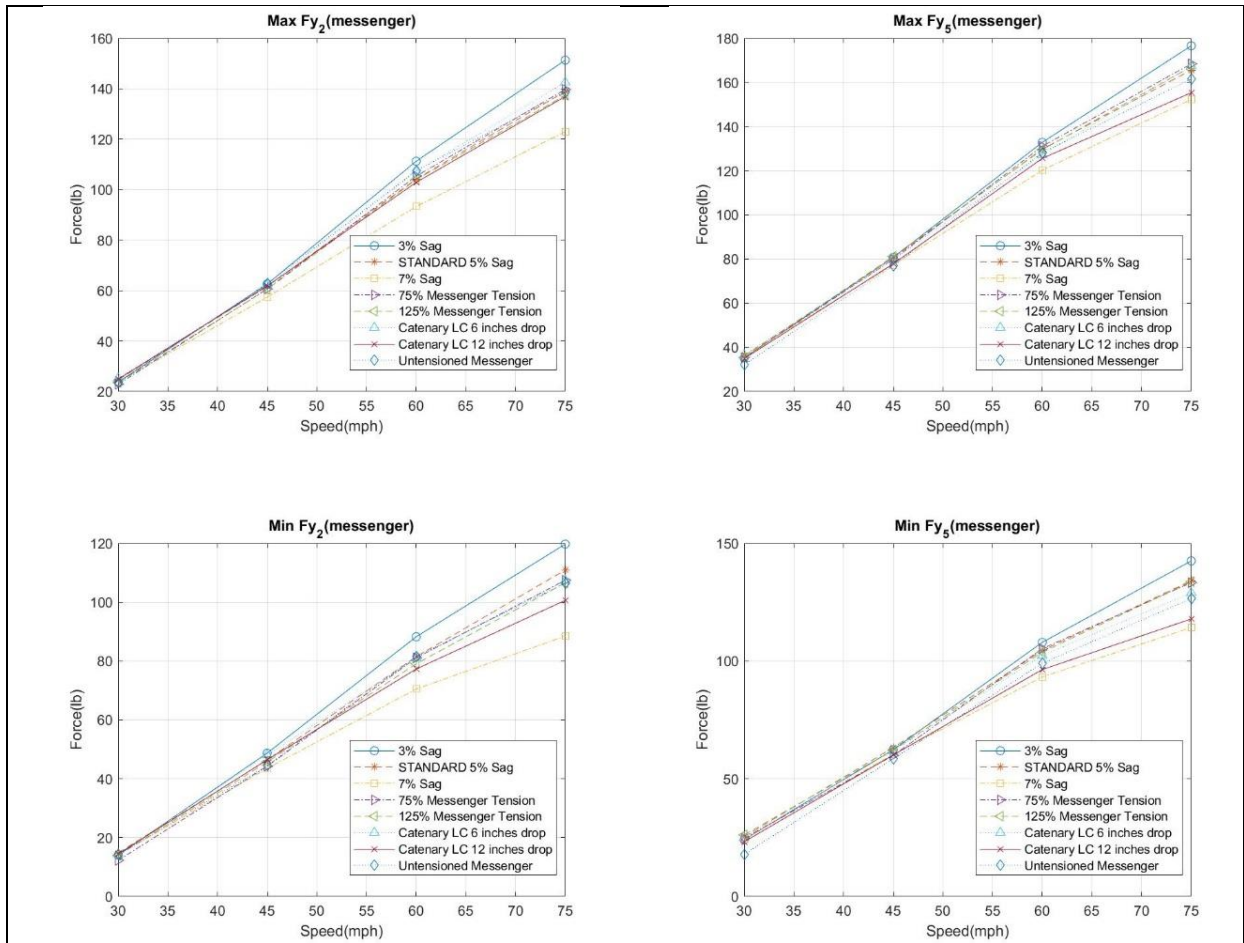


Figure 3-7 - Maximum & minimum messenger wire drag forces

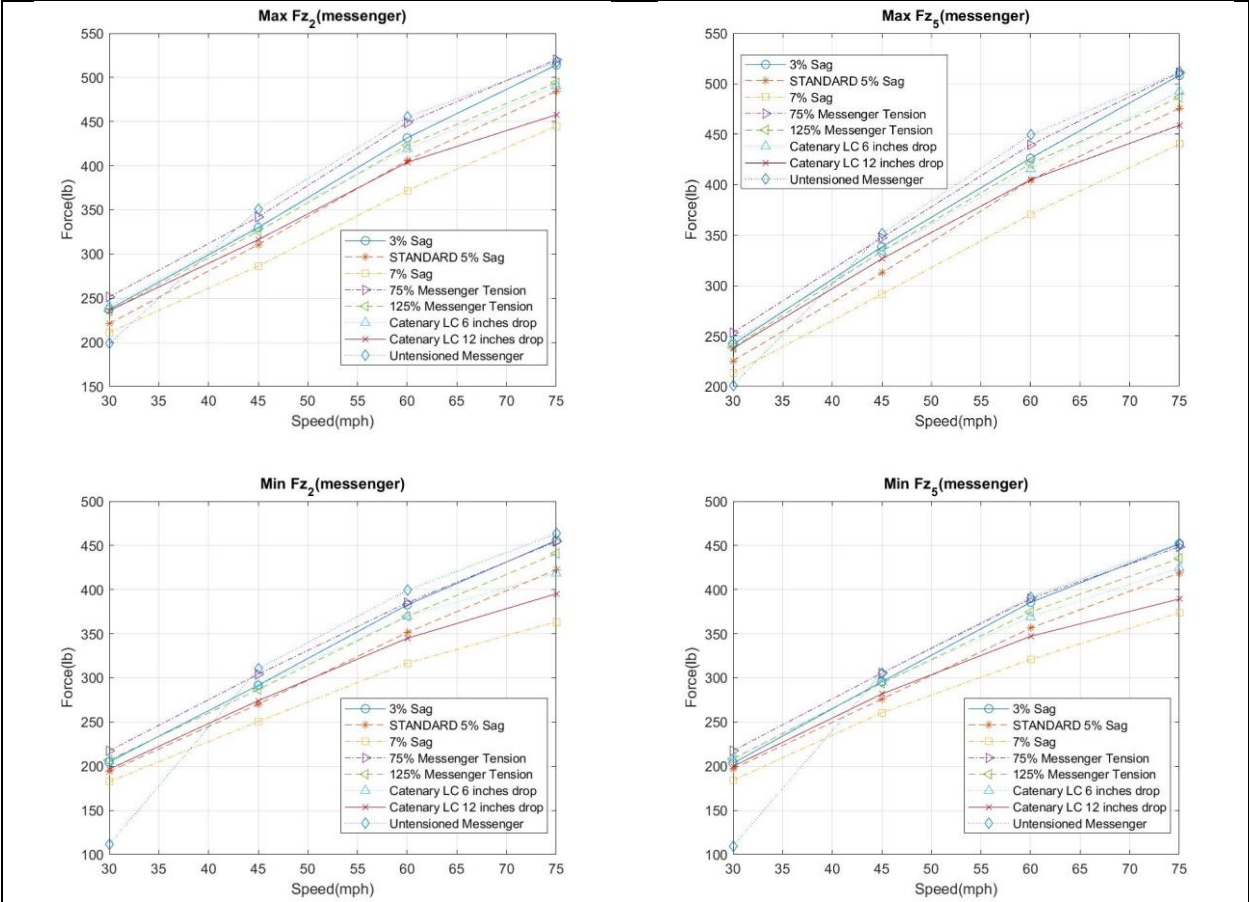


Figure 3-8 - Maximum & minimum messenger wire tension forces

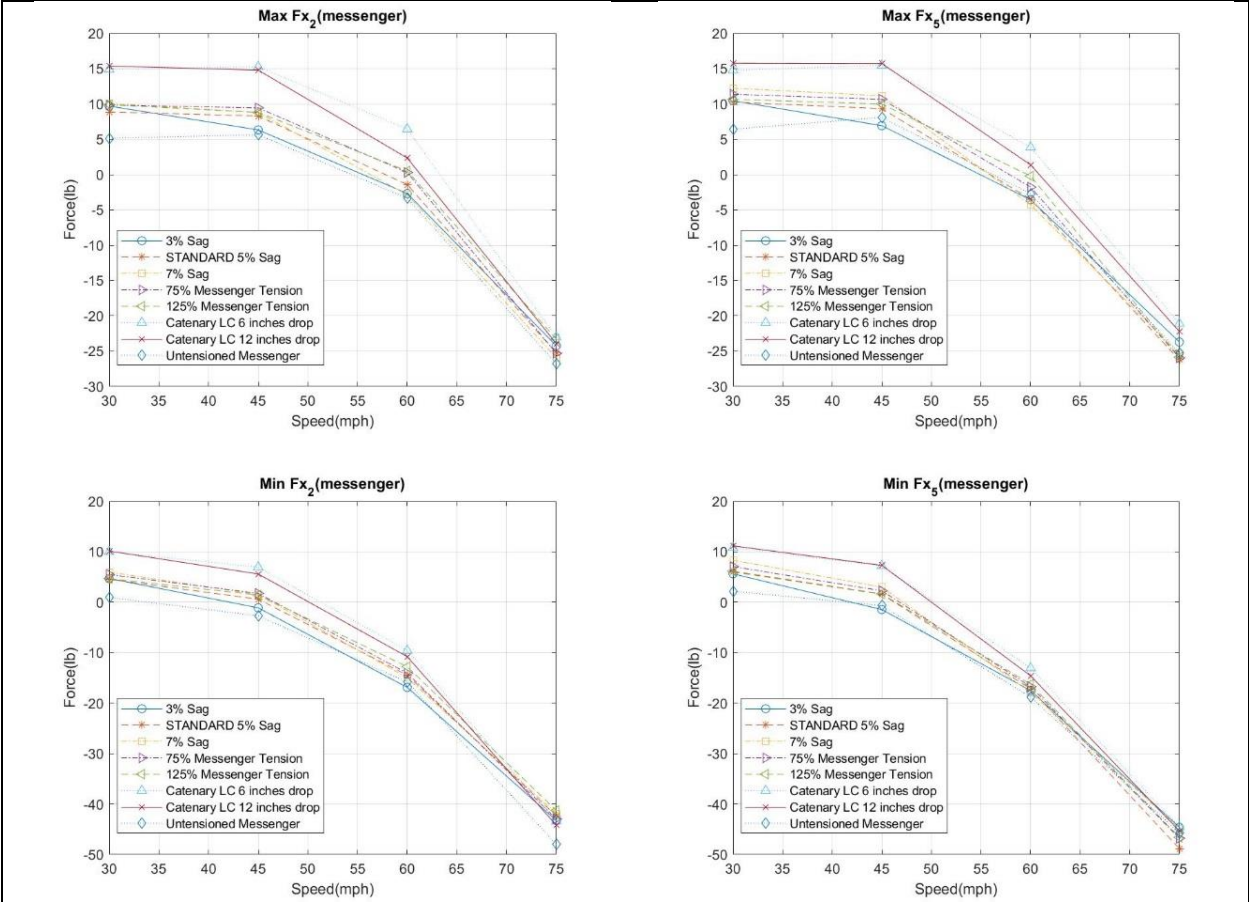


Figure 3-9 - Maximum & minimum messenger lift forces

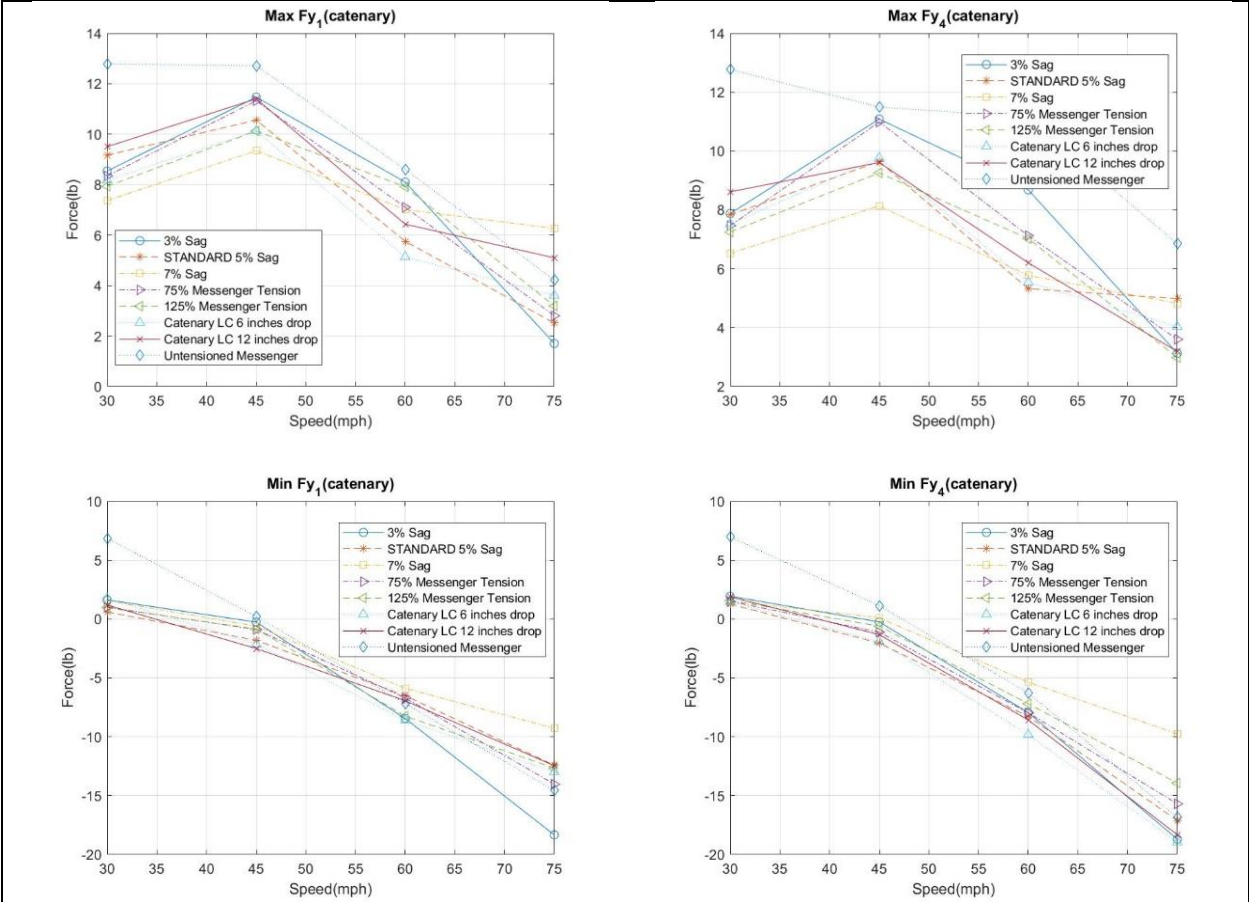


Figure 3-10 - Maximum & minimum catenary drag forces

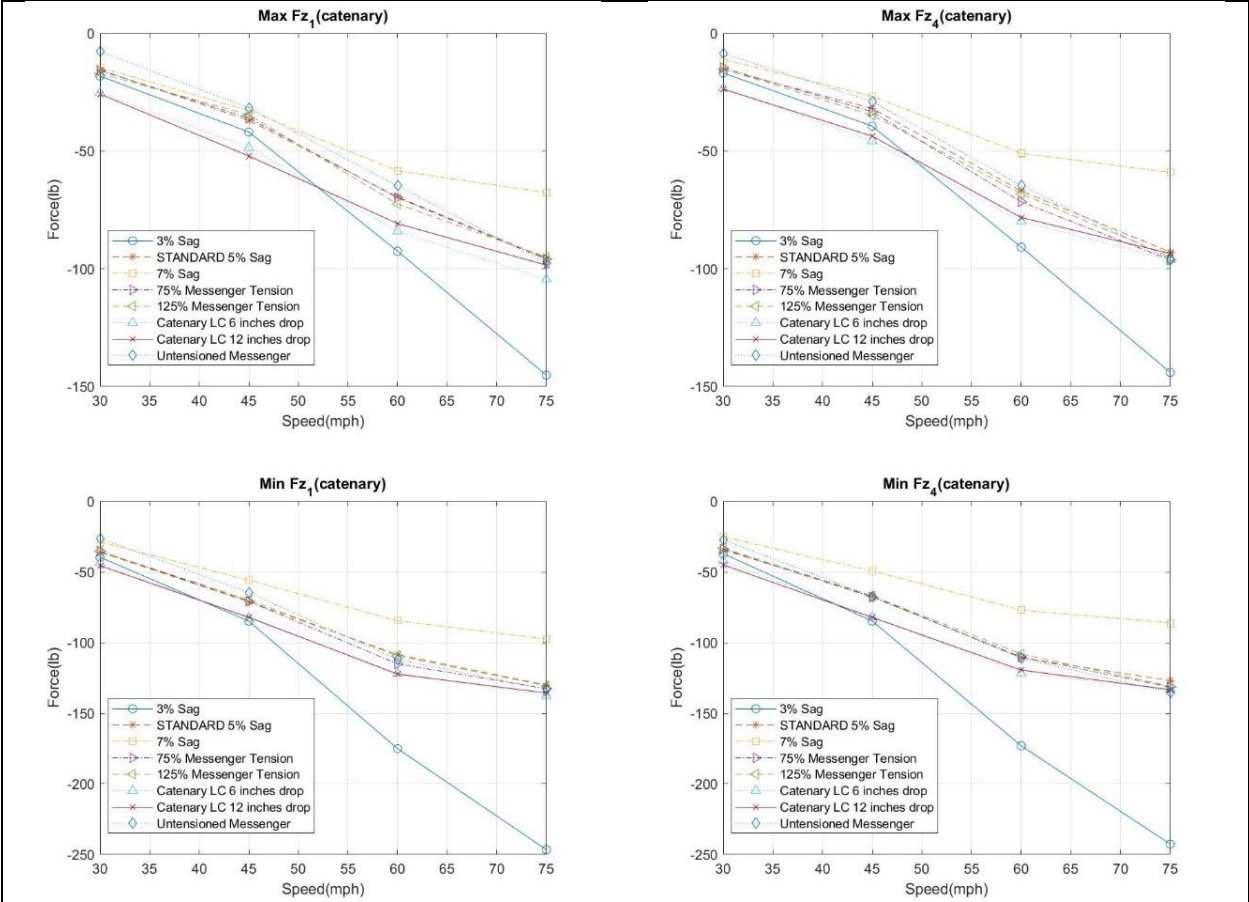


Figure 3-11 - Maximum & minimum catenary tension forces

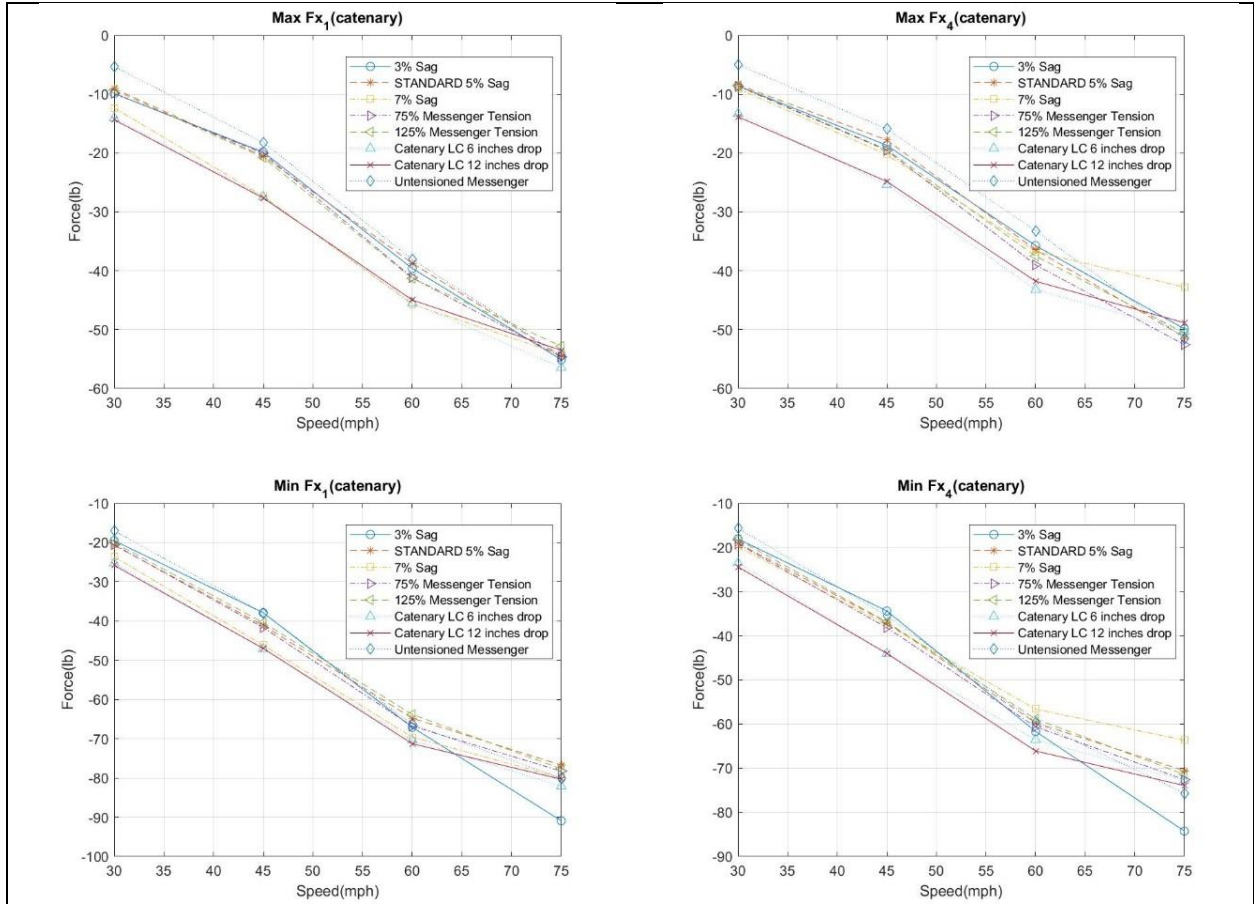


Figure 3-12 - Maximum & minimum catenary lift forces

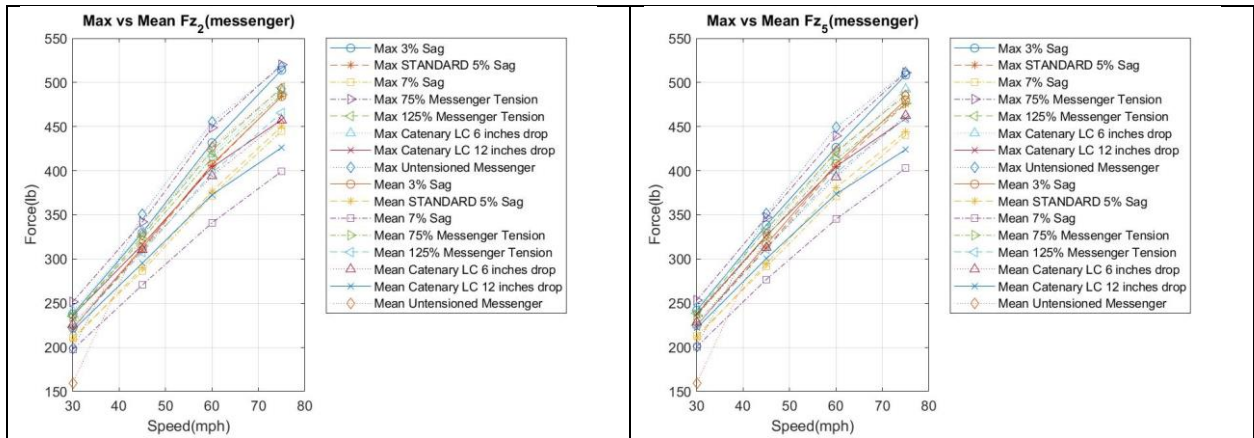


Figure 3-13 - Maximum vs mean messenger tension forces

3.2 RMS of Accelerations

The RMS accelerations are presented in this section. For the 5-section signal (Figure 3-14) the RMS accelerations increased in all cases as wind speed was increased. The difference in RMS of accelerations among the highest and lowest case was of about 20 in/s², at 75 MPH. The RMS accelerations of the 3-section signal also increased with increasing wind speed and the difference among all cases was of about 10 in/s², as shown in Figure 3-15. RMS accelerations from 5-section signal resulted in some slightly lower values that may be due to the higher weight of the 5-section signal compared with the 3-section signal. The 7%-Sag case showed the lowest RMS of accelerations for both, 5-section and 3-section signals while all other cases showed higher RMS accelerations. In any case, the lower wind speeds considered here did not generate any aerodynamic instabilities therefore the RMS accelerations were in general low.

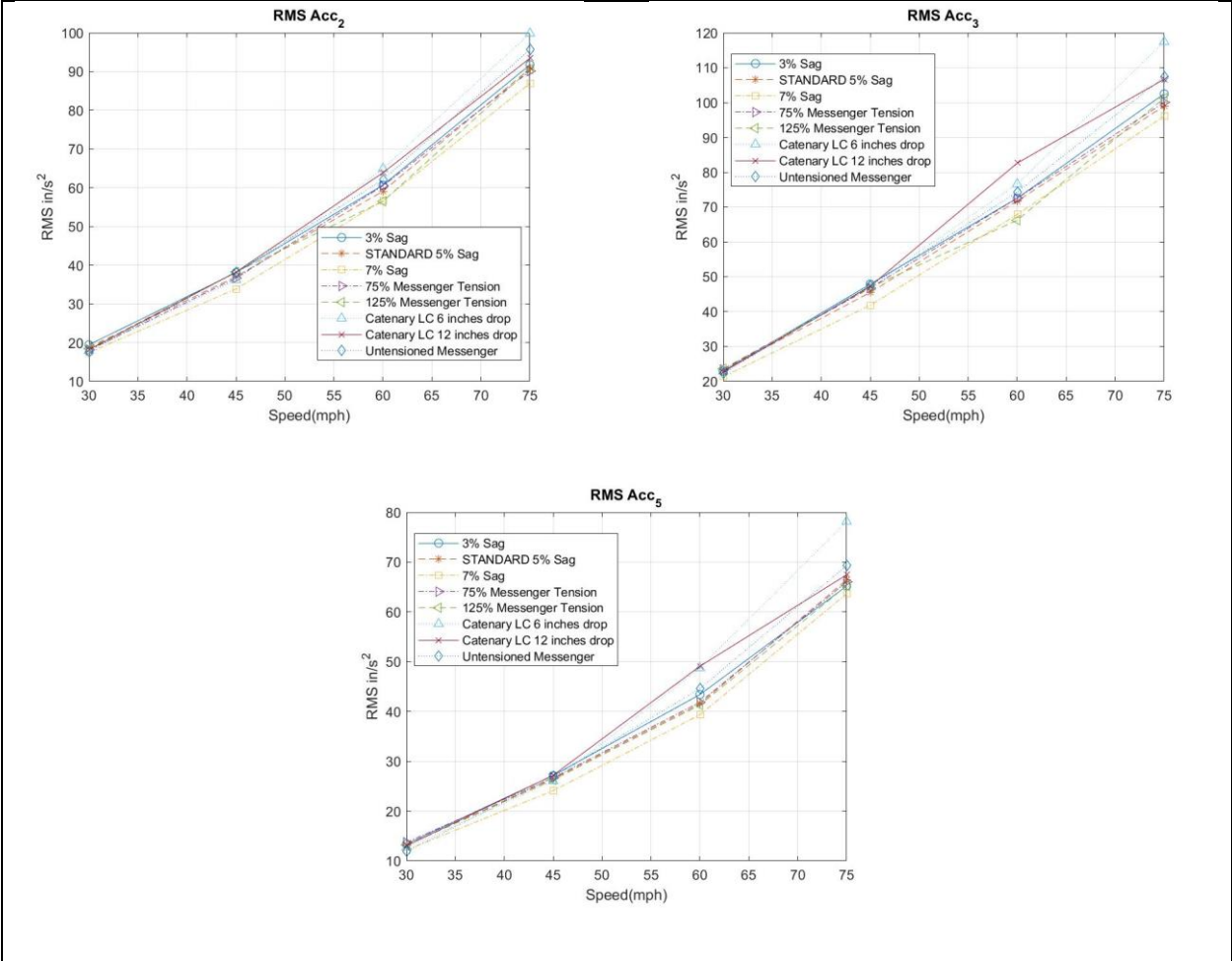


Figure 3-14 - 5-section signal RMS of accelerations

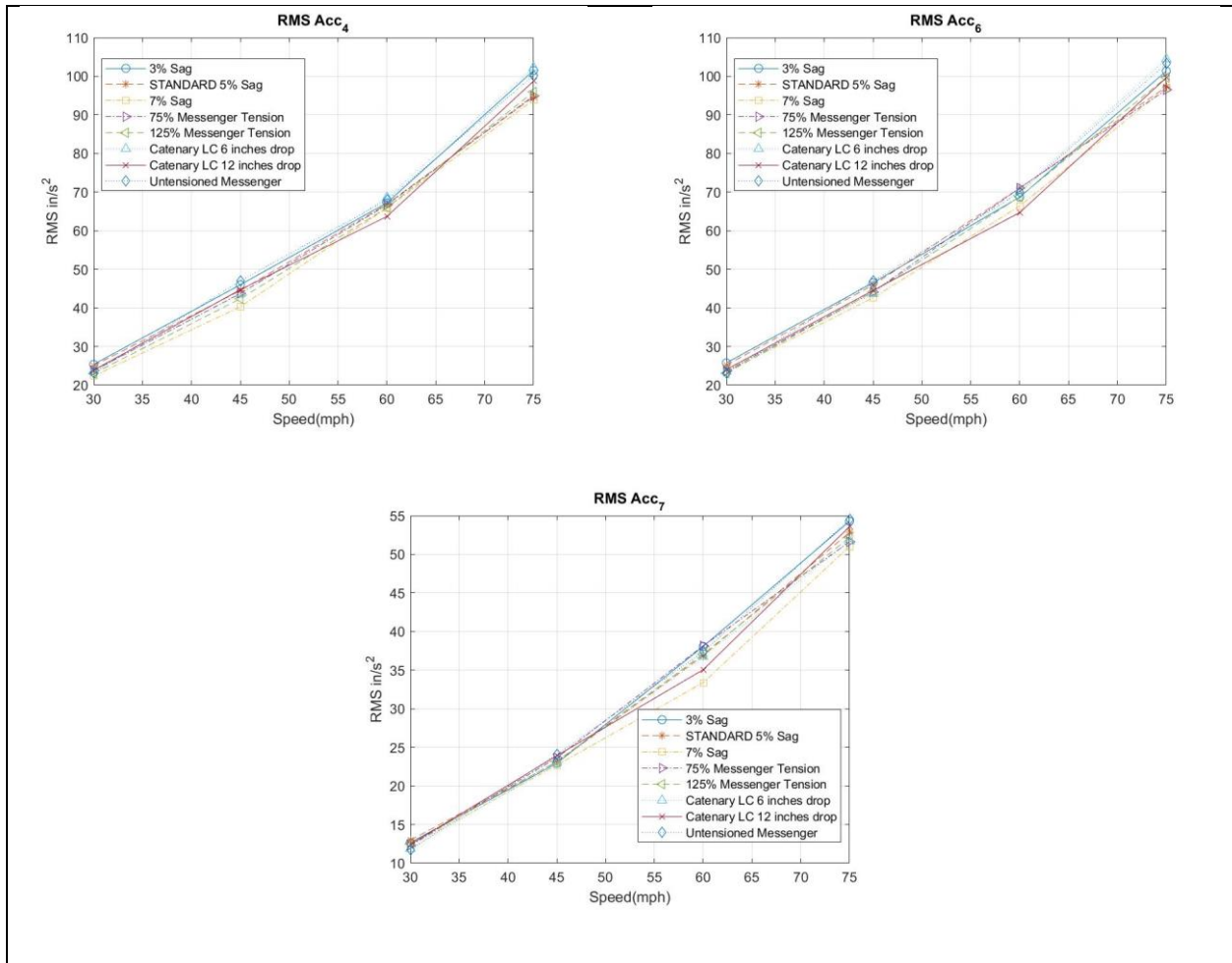


Figure 3-15 - 3-section signal RMS of accelerations

3.3 Inclinations of the Traffic Signals

Inclinations experienced by the traffic lights are presented in this section. It may be noted that all inclinometers measured inclinations in the along and across wind directions. The location of each inclinometer is shown in Figure 2-18 and Figure 2-19.

It was found that, for all cases, the traffic lights showed an increase in along wind inclinations as wind speed was increased, as shown in Figure 3-16. The comparison of mean inclinations for all tested cases, shows that the 3%-Sag case experienced somewhat lower inclinations than the other cases, while the 7%-Sag and LC-12-inches-

drop-down cases underwent higher inclinations for the 5-section signal. When looking at the behavior of the east 3-section signal, it was found that the case giving the least inclinations was the 125%-tension case while the highest inclinations was recorded with the 7%-Sag case, as shown in the bottom graphs of Figure 3-16. It needs to be noted that the difference between all cases in terms of mean inclinations is very small. For 0 degrees wind direction the mean across wind inclinations are small attaining a value ranging from 0 to 11 degrees, as shown in Figure 3-17.

When looking at the maximum and minimum inclinations, it was found that the 5-section signal maximum inclination was about 65 degrees, during the LC-12-inches-drop-down case at 75 MPH, as shown in Figure 3-18. For the 3-section signal, the maximum along-wind inclination attained a value of about 63 degrees during the untensioned-messenger case at 75 MPH, as shown in Figure 3-19.

Previous work states that when traffic lights incline more than 27 degrees, along the motorist frontal view, the motorists have trouble distinguishing between green, yellow and red light (Cook et al, 2012). It is because of this reason that FDOT considers an inclination of more than 27 degrees as non-functional, as it produces safety concerns. As it can be seen from Figure 3-16, the lights undergo inclinations of more than 27 degrees at speeds greater than 50 MPH.

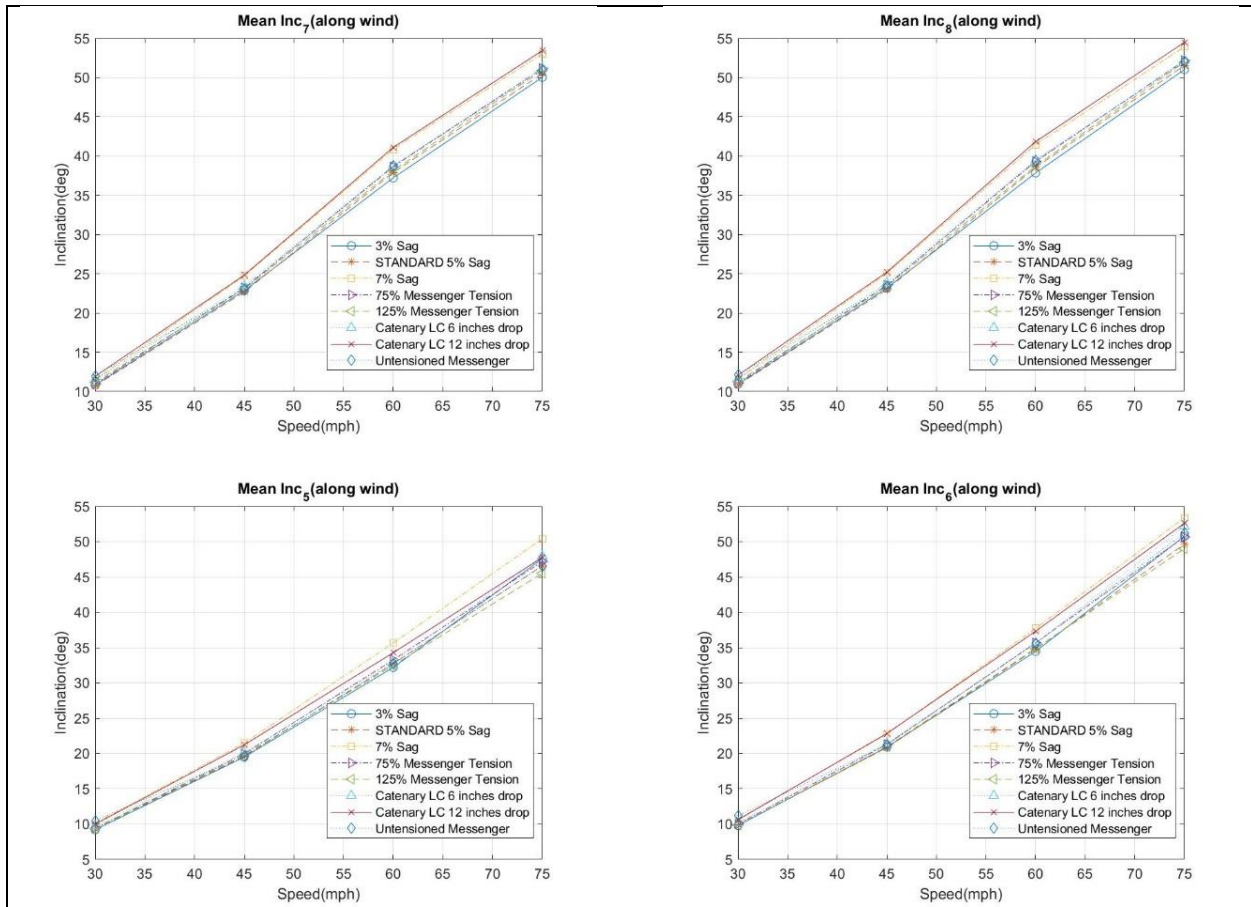


Figure 3-16 - Mean along wind inclinations (Inc 7 and 8 at 5-section signal & Inc 5 and 6 at 3-section signal)

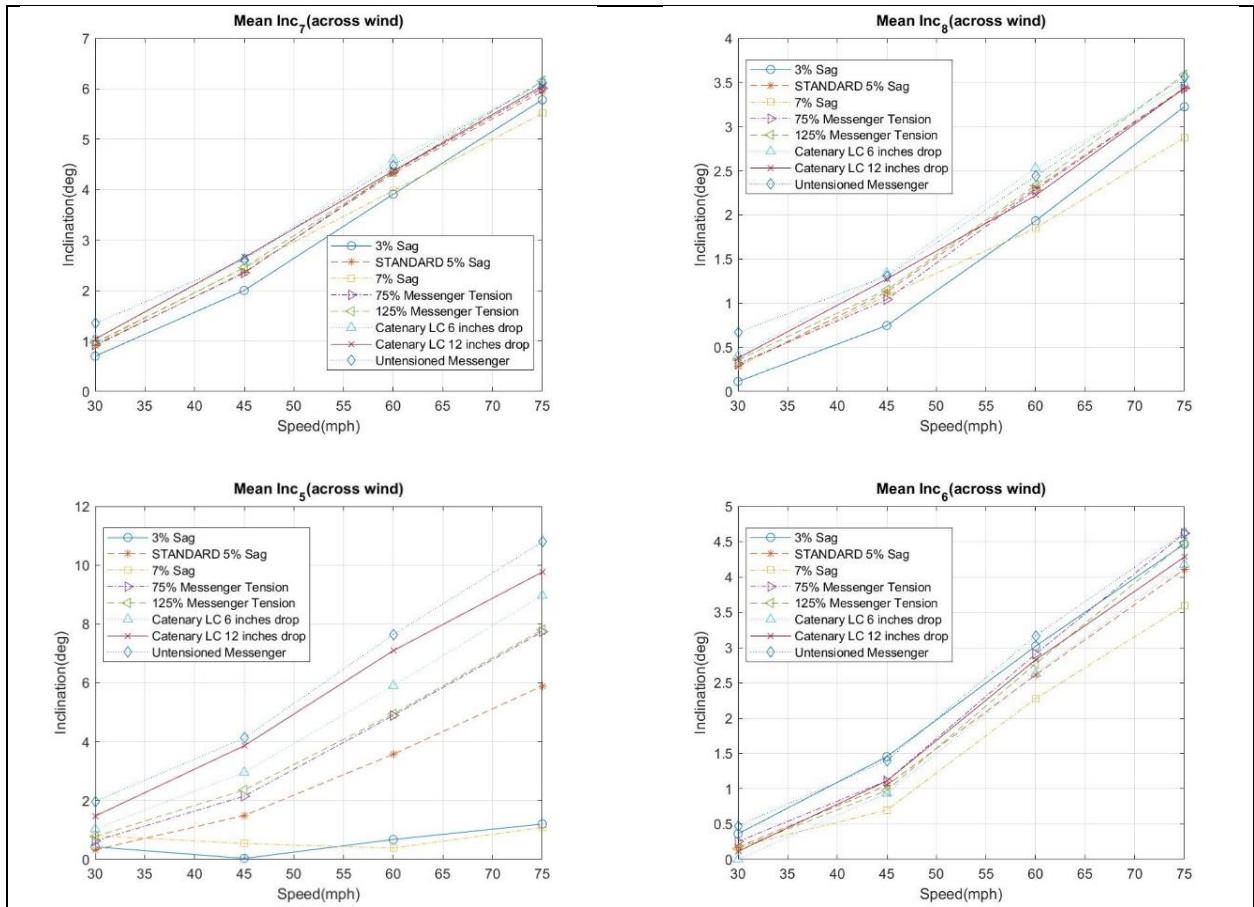


Figure 3-17 - Mean across wind inclinations (Inc 7 and 8 at 5-section signal & Inc 5 and 6 at 3-section signal)

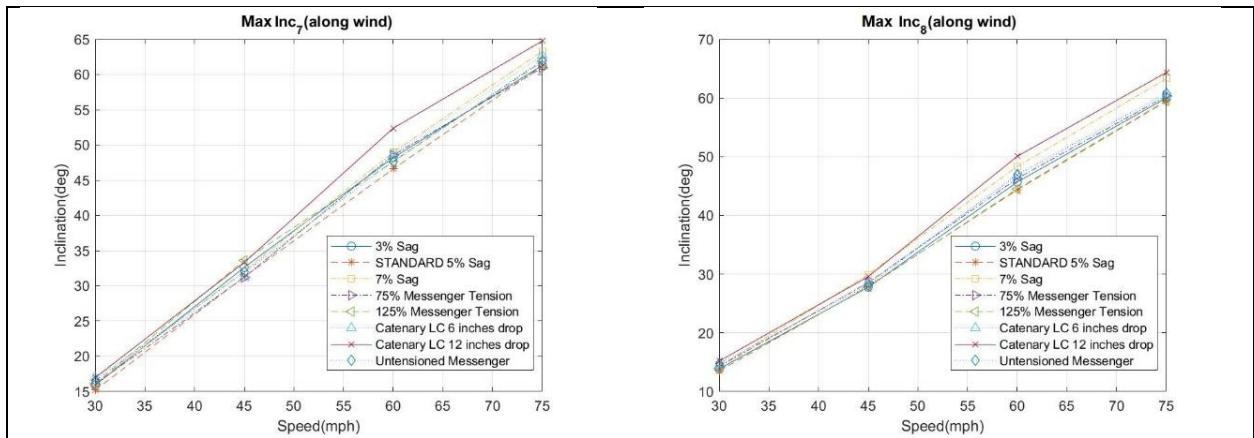


Figure 3-18 - 5-section signal maximum inclinations along wind

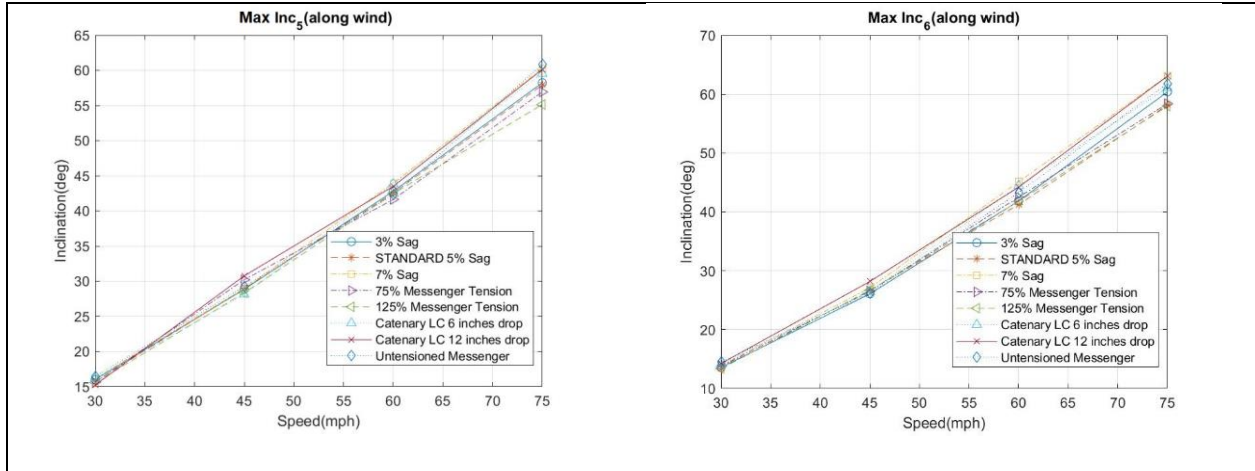


Figure 3-19 – 3-section signal maximum inclinations along wind

3.4 Drag Coefficients

The drag coefficient is a non-dimensional quantity that is defined as the ratio of the drag force to the mean dynamic pressure times the reference area exposed to the wind field. To calculate the drag coefficient resulting from the tests performed at the different wind speeds and wind angles of attack, the drag force must be determined by adding all the drag forces measured by the load cells for each test and divide it by the mean dynamic pressure multiplied by the frontal area. The drag coefficient is defined as:

$$C_D = \frac{F_D}{\frac{1}{2} \rho V^2 A} \quad \text{Equation 1}$$

where F_D is the total drag force, ρ is the air density, V is the mean wind speed at the mean height of the traffic light assembly, and A is the total frontal area. In all cases the total frontal area is the sum of one 5-section signal, two 3-sections signals, coil springs, hangers, shackles and turn buckles, which attained a value of 30.7 ft².

To account for the default units used by the WOW instrumentation, the formula should be modified as follows:

$$C_D = \frac{F_D}{0.00256V^2A} \quad \text{Equation 2}$$

with drag force (F_D) measured in lbs, wind velocity (V) measured in MPH and area (A) measured in ft^2 .

The resultant drag force (F_D) for each case was taken by adding all the contributions of along wind force of all load cells, that is 2 load cells measuring forces of the messenger wire and 2 load cells measuring forces of the catenary wire. The area utilized for calculating the drag coefficients (C_D) was the addition of the total frontal area, as previously stated. The drag force produced by the cables was neglected as the drag force generated by them is assumed to be relatively small (Xu Xie et al., 2014).

The velocities used to calculate the drag coefficient (C_D) were the estimated velocities at the mean height of the traffic light assembly. As previously mentioned, there is a pitot tube installed at 10.5 feet above the test floor and just about the exit of the flow management system of the WOW. The height from the surface of the turn table to the center of the traffic lights was calculated to be about 64 inches. For this reason, the power law was utilized to calculate the wind velocity at the center of the traffic lights.

As it can be seen in Figure 3-20, The drag coefficient of the traffic light assembly had small changes for wind speeds of 30 and 45 MPH. At wind speeds greater than 45 MPH, the drag coefficient decreased as wind speed is increased. After 45 MPH, the case that resulted in higher drag coefficients was the 3%-Sag case, while the case giving the lowest drag coefficients was the 7%-Sag case. The worst drag coefficient was measured at 30 MPH during the untensioned-messenger case, attaining a value of 1.09. For the 3%-Sag

case, the drag coefficient at 45 MPH was found to be 1.05 and at 75 MPH it was found to be 0.757. AASHTO, LRFD Specifications for Structural Supports for Highway Signs, Luminaires, and Traffic Signals (2015) suggest using a drag coefficient (C_D) of 1.20 (Table 3.8.7-1). Experiments done at University of Florida have performed a similar research utilizing one single 5-section signal and have stated that the drag coefficient of a single 5-section traffic signal mounted on a single cable should be 0.7 (Cook et al., 2012).

It needs to be noted that at 180 degrees, the drag coefficients are higher than at 0 degrees, as shown in A: 26, where the case resulting in higher drag coefficients was the 3%-Sag assembly attaining a value 1.67 at 30 mph and 0.98 at 75 mph. The overall behavior remains the same as the one at 0 degrees, thus drag coefficient decreasing with increasing speed and 7%-Sag assembly giving the lowest drag coefficient values.

If the traffic lights could be idealized as a solid flat plate, the same drag coefficients should be expected at angles of attack of 0 degrees and 180 degrees, however, results show that the drag coefficients are higher at 180 degrees, as previously stated. As it can be seen in Figure 3-21 and Figure 3-22, the drag coefficients decreased as the inclination of the traffic lights is increased. The figures show a good correlation between the behavior of the span-wire system at 0 and 180 degrees wind angle of attack and it can be concluded that there are aerodynamic effects influencing the results of drag coefficients as the specific shape of each case, at different wind angles of attack, is affecting the aerodynamics of the traffic lights.

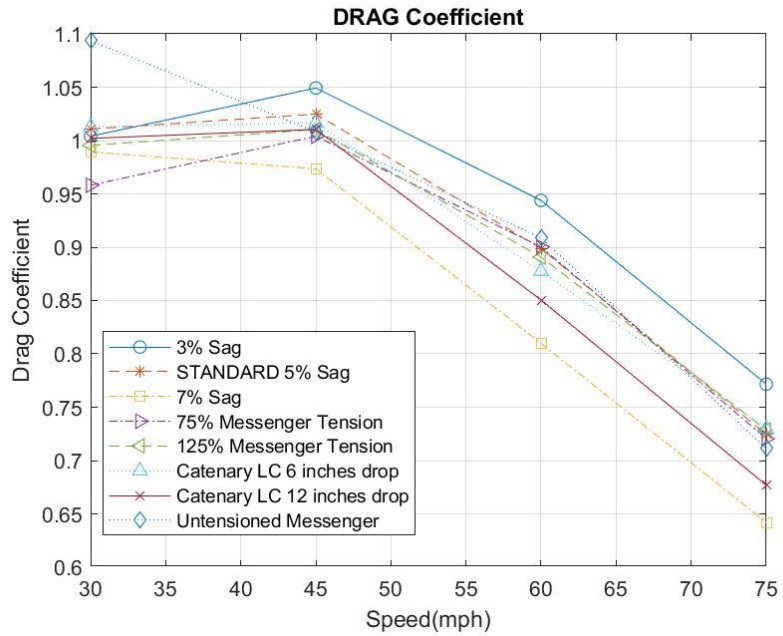


Figure 3-20 - Drag coefficients vs wind speed

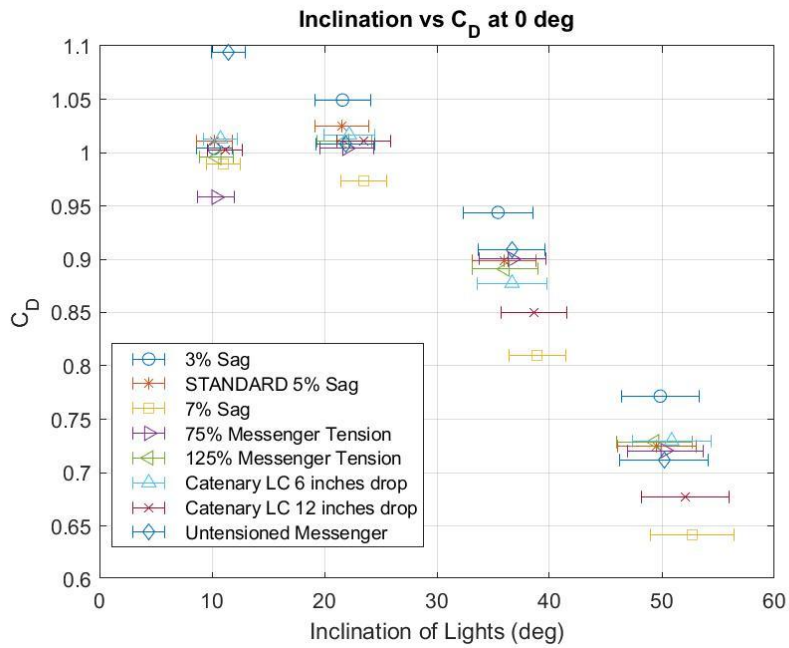


Figure 3-21 - Mean inclinations of traffic signals vs drag coefficients with standard deviation at 0 degrees wind angle of attack

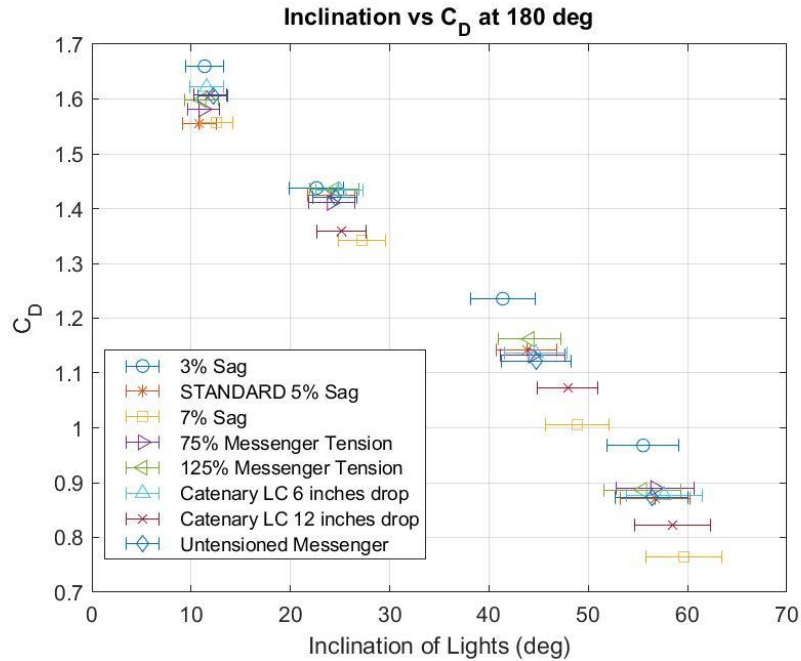


Figure 3-22 - Mean inclinations of traffic signals vs drag coefficients with standard deviation at 180 degrees wind angle of attack

3.5 Lift Coefficients

The lift coefficient expresses the ratio of the lift force to the force produced by the mean dynamic pressure over the effective area. To calculate the lift coefficient at different wind speeds and wind angles of attacks, the lift force must be determined by adding all the lift forces measured by the load cells for each test and then divided by the dynamic pressure multiplied by the top view area of the traffic lights. The lift coefficient is defined as:

$$C_L = \frac{F_L}{\frac{1}{2} \rho V^2 A} \quad \text{Equation 3}$$

where F_L is the lift force, ρ is the air density, V is the mean wind speed and A is the top view area of two 5-section signals and one 3-section signals and resulted to be 10.3 ft².

To account for the default units used by the WOW instrumentation, the formula should be modified as follows:

$$C_L = \frac{F_L}{0.00256V^2A} \quad \text{Equation 4}$$

with lift force (F_L) measured in lbs, wind velocity (V) measured in MPH and area (A) measured in ft^2 .

The resultant lift force (F_L) for each case was taken by adding all the contributions of x component of all load cells, that is 2 load cells measuring forces of the messenger wire and 2 load cells measuring forces of the catenary wire, as seen in Figure 2-3. It needs to be noted that the direction in the x component of all load cells was adjusted to be of negative sign in the downward direction. The area utilized for calculating the lift coefficients (C_L) was the addition of the top view area of one 5-section signal, two 3-section signals, turn buckles, springs and shackles. The velocities used to calculate the lift coefficient (C_L) are the calculated velocities at the center of the traffic light assembly. The mean wind speed at mean signal height was estimated using the same approach as that described in the drag coefficient section.

As it can be seen in Figure 3-23. The lift coefficient values of the traffic light assembly increased linearly up to 60 MPH after which they keep increasing at a much lower rate. From all cases tested, it was found that for speeds less than 60 MPH, the 7%-Sag case gives the highest lift coefficient value. After 60 MPH, the 7%-Sag case lift coefficient decreased the incremental rate to a negative slope. At 75 MPH, the case giving the worst lift coefficient is the 3%-Sag case, attaining a maximum value of about 1.7 and the case

giving the least lift coefficient at 75 MPH is the 7%-Sag case, attaining a value of about 1.59. AASHTO LRFD Specifications for Structural Supports for Highway Signs, Luminaires, and Traffic Signals (2015) does not give any suggestion for lift coefficients. It needs to be noted that at 180 degrees, the lift coefficients have a higher magnitude than those found at 0 degrees. The highest lift coefficient during the 180 degrees test was found to be 2.2 approximately at 60 MPH which decreases as wind speed is increased to 75 MPH, as shown in A: 27. The overall trend of the 180 degrees test is similar to that of the 0 degrees test, as the lift force increases as wind speed is increased, except for the lift coefficients found after 60 MPH.

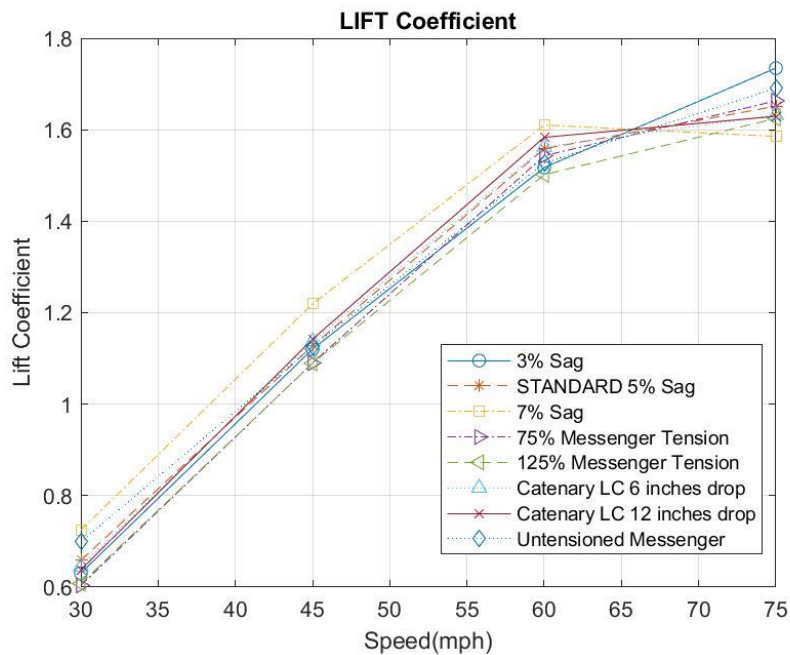


Figure 3-23 - Lift coefficients vs wind speed

4. Conclusion

In the past, traffic signals mounted on span-wire systems have experienced significant damages during extreme wind events causing unfavorable situations during and after an extreme wind event. To ensure a better design and enhance the survivability and sustainability of these systems, experiments were performed at the Wall of Wind (WOW) experimental facility located in Florida International University (FIU). Different parameters of the assembly were modified to assess their effect on the overall performance of the traffic signal assemblies. The different tested cases were the FDOT-standardized assembly, 7%-Sag assembly, 3%-Sag assembly, 75%-messenger-tension assembly, 125%-messenger-tension assembly, 6-inch-drop-down of catenary load cells assembly, 12-inch-drop-down of catenary load cells assembly and untensioned-messenger assembly. Wind velocities were gradually increased from 30 to 75 MPH at angles of 0, 45, 135 and 180 degrees. The forces (drag, lift and tension) were measured by load cells, inclinations were measured by inclinometers and accelerations were measured by accelerometers. Overall, the wind-induced forces increased with increasing wind speed. Results show that the assembly that resulted in the lowest mean forces of lift, tension and drag, was the 7%-Sag assembly while the 3%-Sag assembly resulted in higher forces. For the maximum lift, drag and tension forces, the 7%-Sag case gave lower forces among all eight cases while the 3%-Sag, 75%-messenger tension and 6-inch-drop-down cases gave somewhat higher values among all eight cases. RMS of accelerations increased with increasing wind speed for all cases and the case that resulted in lower RMS of accelerations was the 7%-Sag assembly. Inclinations of traffic lights assemblies

increased with increasing wind speed. The inclinations of the assemblies are important as excessive inclinations produce visibility issues. Among all eight cases, the higher mean inclinations were experienced by the 7%-Sag and 12-inch-drop-down cases while the case giving the least inclinations was the 3%-Sag assembly; however, the difference between results is of about 5 degrees. For all tested cases the drag coefficients decreased as wind speed was increased. For 0 degrees wind direction, the highest drag coefficient was the untensioned-messenger case (1.09) at 30 MPH and the 3%-Sag (0.77) at 75 MPH. The case that resulted in the lowest drag coefficients, for all but one wind speed, was the 7%-Sag assembly while the case giving the higher drag coefficients, for all but one wind speed, was the 3%-Sag assembly. Lift coefficients were found to increase as wind speed is increased. The case that produced the higher lift coefficient was the 3%-Sag assembly at 75 MPH. However, before 75 MPH, the 7% Sag assembly gave higher lift coefficients among all eight cases. It was found that at 180 degrees wind angle of attack, the drag and lift coefficients are even greater than those found at 0 degrees, attaining a maximum value of 1.67 and 2.2 among all tested cases, respectively. Results show that traffic signals mounted on a span-wire system performed better with a catenary wire sag of 7%. Nevertheless, it is recommended to test this configuration at higher speeds to see the overall response under wind speeds greater than 75 MPH and identify if aerodynamic instabilities develop.

References

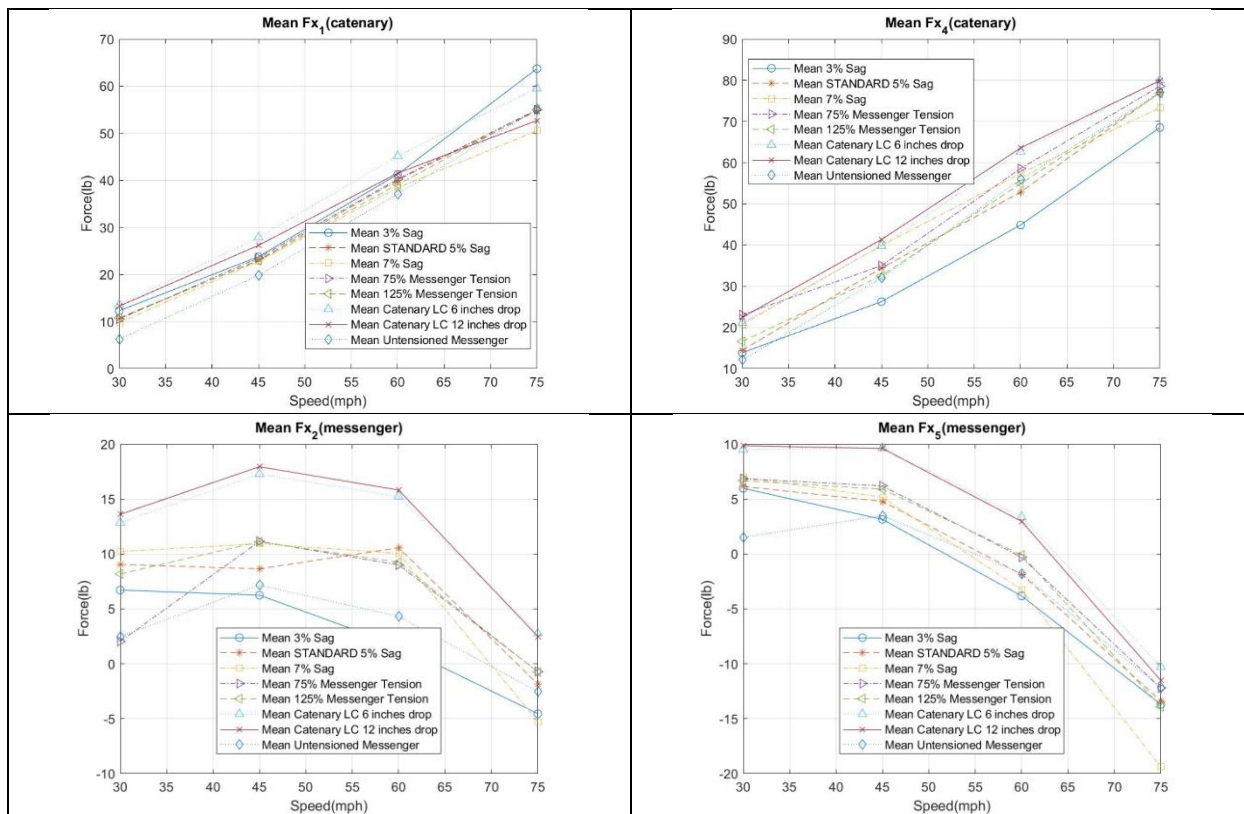
1. Aly, A. M., Chowdhury, A. G., Bitsuamlak, G. (2011) "Wind profile management and blockage assessment for a new 12-fan Wall of Wind facility at FIU", *Wind & Structures*, 14(4), 285-300.
2. B. Berlanga, I. Zisis, A. G. Chowdhury, P. Irwin, A. Azzizinamini, research project BOV29 TWO 977-20, FIU, 2015.
3. Chowdhury, A.G., Zisis, I., Irwin, P., Bitsuamlak, G.T., Pinelli, J.P., Hajra, B., Moravej, M. "Large Scale Experimentation using the 12-Fan Wall of Wind to Assess and Mitigate Hurricane Wind and Rain Impacts on Buildings and Infrastructure Systems", *Journal of Structural Engineering (ASCE)-Special Issue: Recent advances in assessment and mitigation of multiple hazards for structures and infrastructures*, 2016. DOI: 10.1061/(ASCE)ST.1943-541X.0001785.
4. Cook, R.A., Masters, F., & Rigdon, J.L. "Evaluation of Dual Cable Signal Support Systems with Pivotal Hanger Assemblies." FDOT Contract No. BDK75 977-37, University of Florida, Department of Civil and Coastal Engineering, Gainesville, FL, 2012.
5. Florida Department of Transportation Standard Specifications for Road and Bridge Construction, January 2017.
6. Irwin, P., Zisis, I., Berlanga, B., Hajra, B., Chowdhury G. A. Wind Testing of Span-Wire Traffic Signal Systems, Resilient infrastructure, London, June 2016.
7. Kargarmoakhar, R., Chowdhury, A.G., Irwin, P. Reynolds number effects on twin box girder long span bridge aerodynamics, *Wind and Structures*, Vol. 20, No. 2, 2015.
8. Meyer, D., Zisis, I., Hajra, B., Chowdhury, G. A., Irwin, P. "An Experimental Study on the Wind-Induced Response of Variable Message Signs." *Frontiers in Built Environment*. November 2017.
9. Mooneghi, M. A., Irwin, P., Chowdhury, A. G. Large-scale testing on wind uplift of roof pavers, *Journal of wind engineering and industrial aerodynamics*, 2014.
10. Sivarao SK, Esro M, Anand TJ. Electrical & Mechanical Fault Alert Traffic Light System Using Wireless Technology. *International Journal of Mechanical and Mechatronics Engineering*, 2010.
11. State of Florida Department of Transportation (FDOT). (January 2015). Standard Specifications for Road and Bridge Construction, FDOT, Tallahassee, FL.
12. State of Florida Department of Transportation (FDOT), "Hurricane Response Evaluation and Recommendations: February 11, 2005, Version 5." FDOT, Tallahassee, FL. 2005.
13. Xu Xie, Xiaozhang Li and Yonggang Shen, "Static and Dynamic Characteristics of

a long-Span Cable-Stayed Bridge with CFRP Cables”, June 2014.

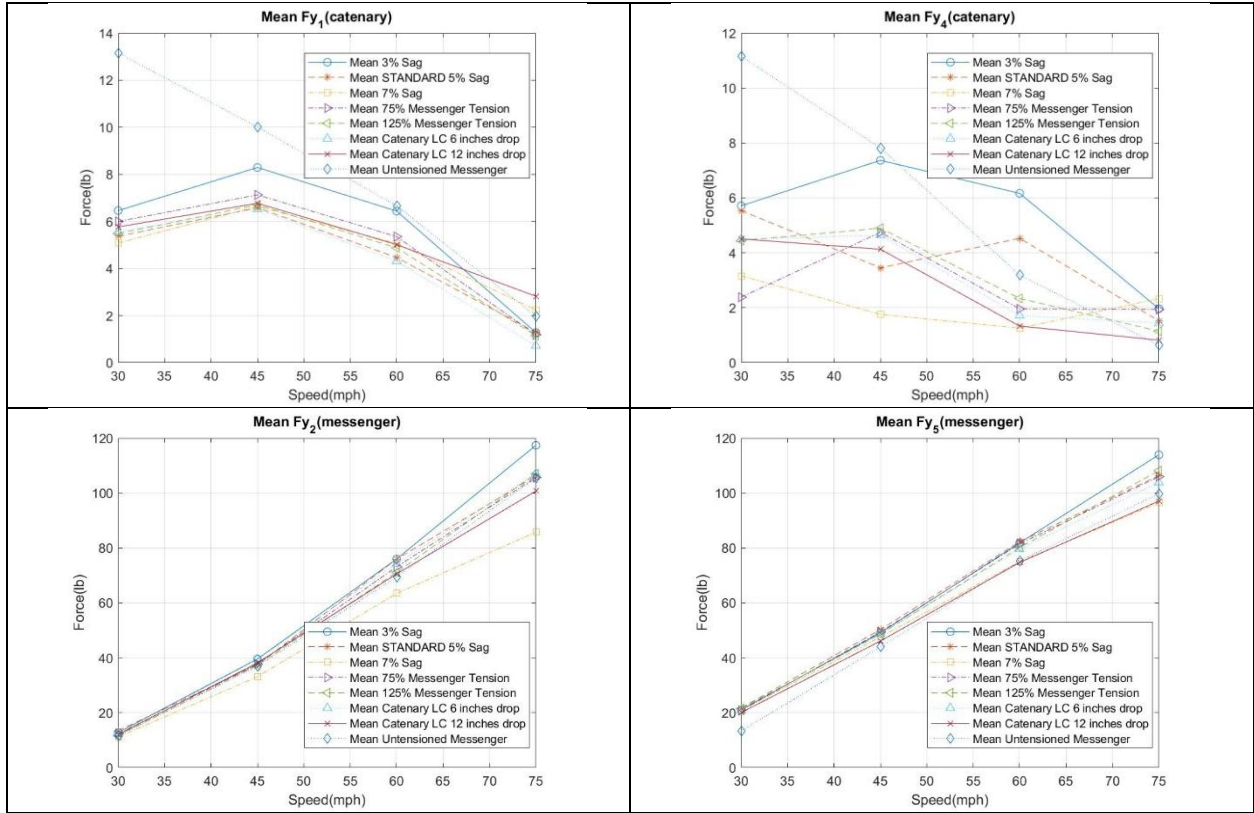
14. Zisis, I., Irwin, P., Berlanga, B., Chowdhury, A.G., Hajra, B. Assessing the performance of vehicular traffic signal assemblies during hurricane force winds”, Proceedings of the 1st International Conference on Natural Hazards and Infrastructure, Chania, Greece, June 2016.

Appendix

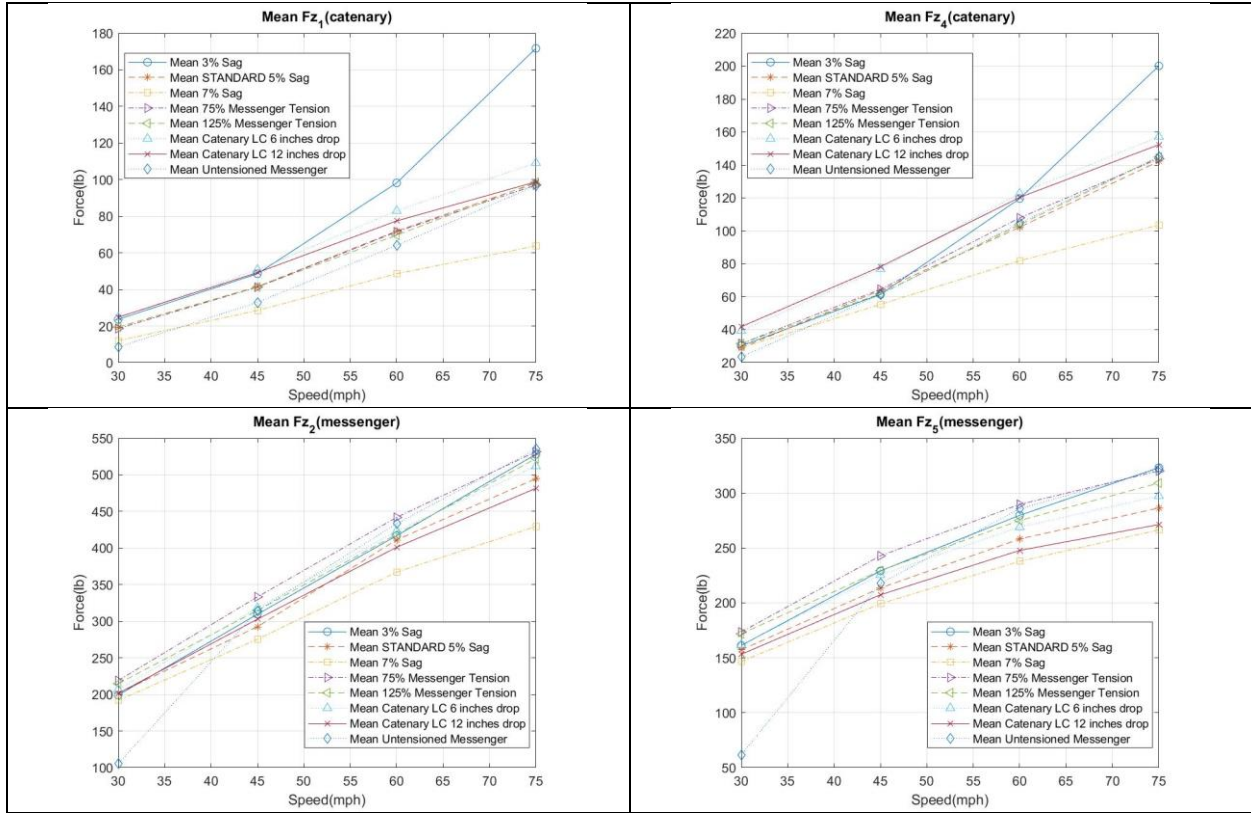
Results for 45 degrees wind angle of attack



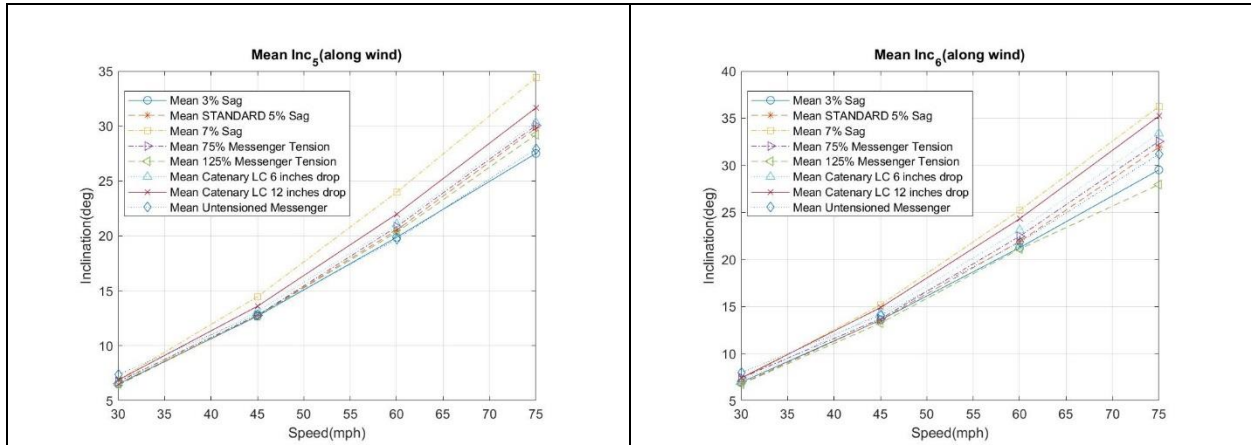
A: 1 - Mean lift forces 45 degrees



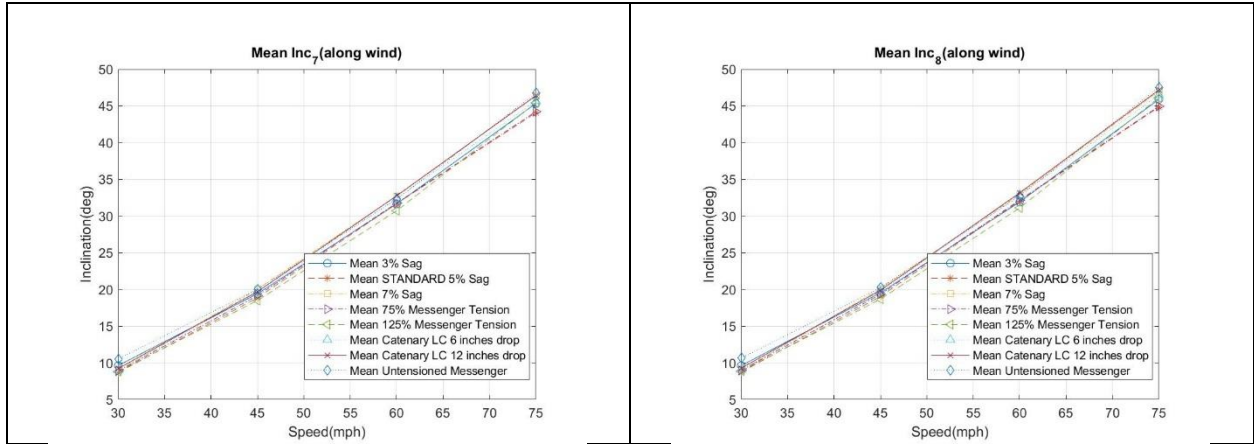
A: 2 - Mean drag forces 45 degrees



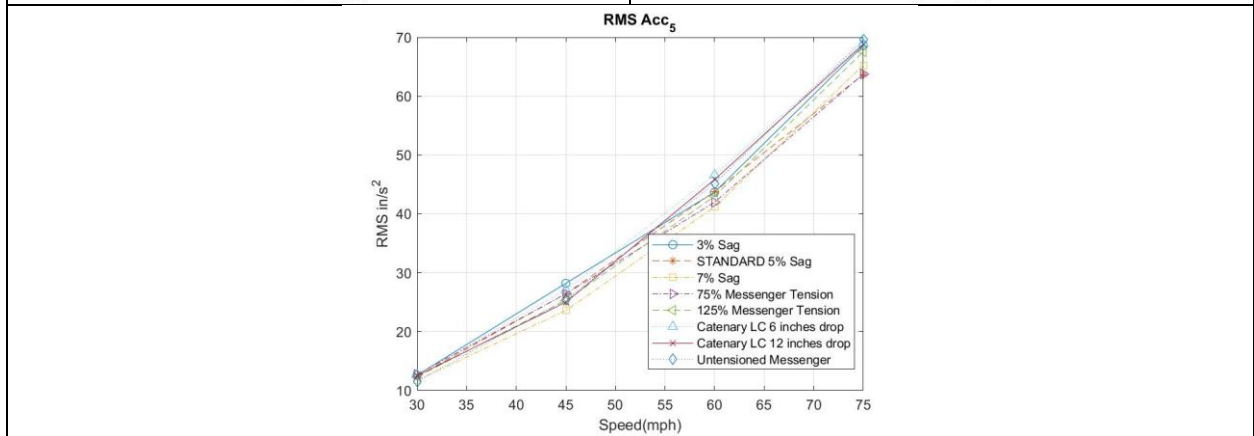
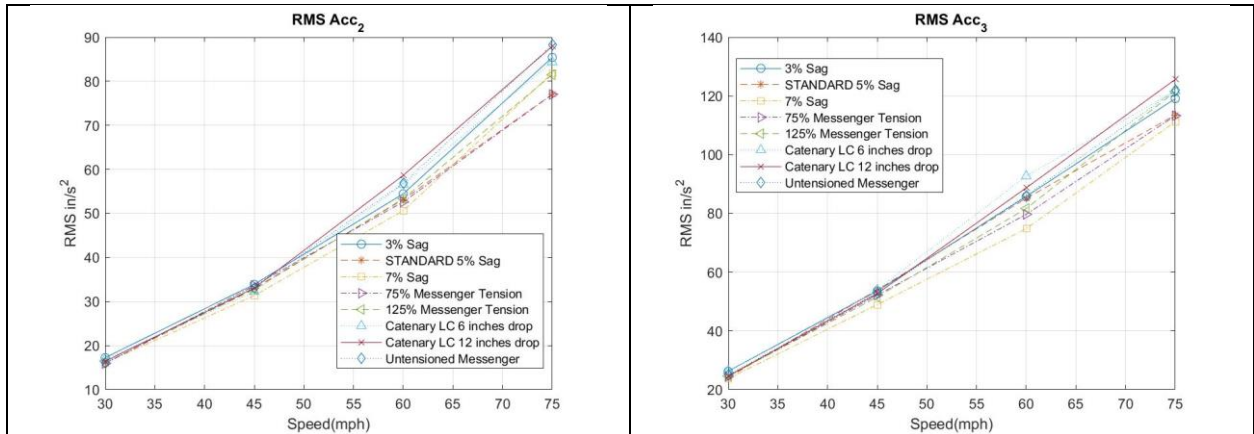
A: 3 - Mean tension forces 45 degrees



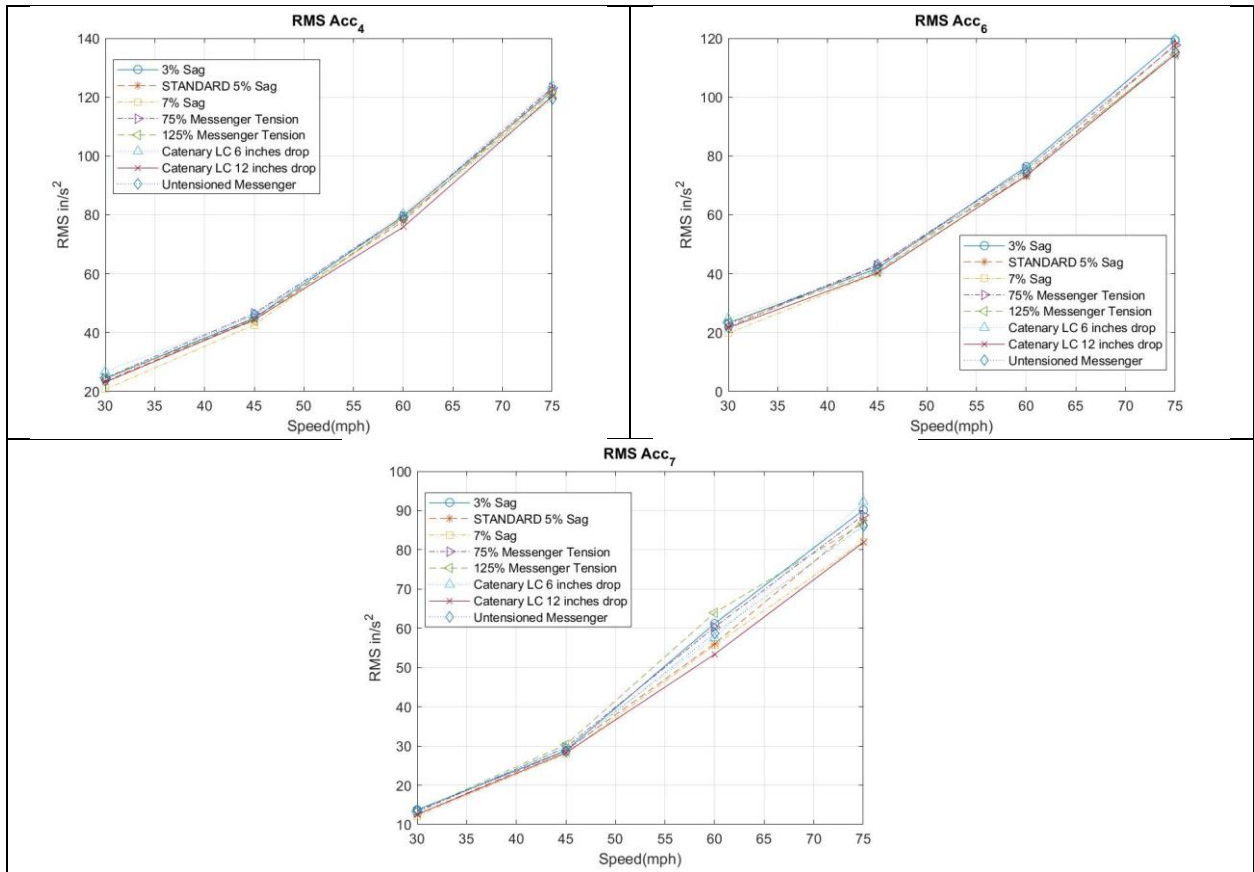
A: 4 - 3-section signal mean inclinations along wind 45 degrees



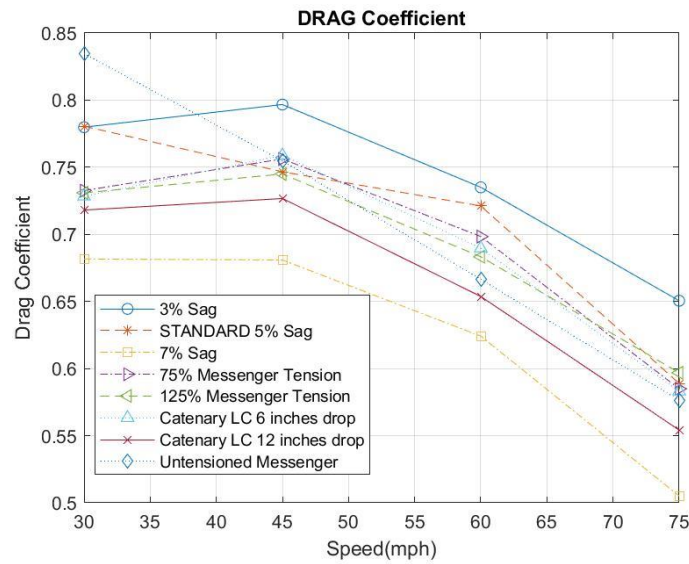
A: 5 - 5-section signal mean inclinations along wind 45 degrees



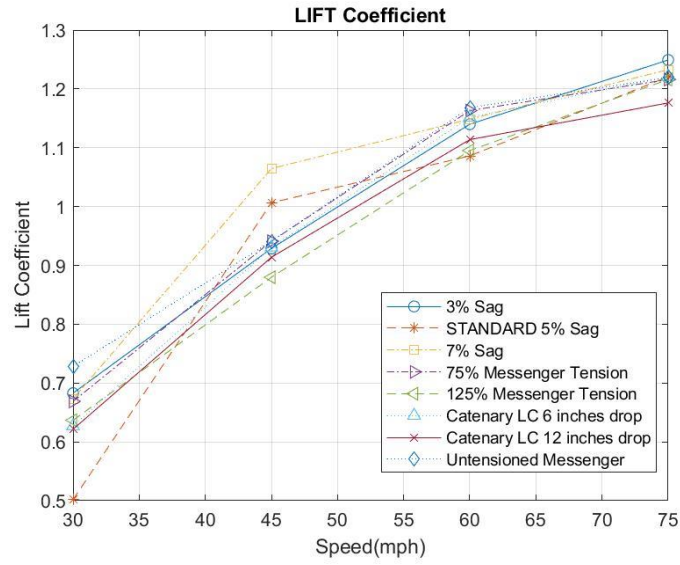
A: 6 - 3-section signal rms of accelerations 45 degrees



A: 7 - 5-section signal rms of accelerations 45 degrees

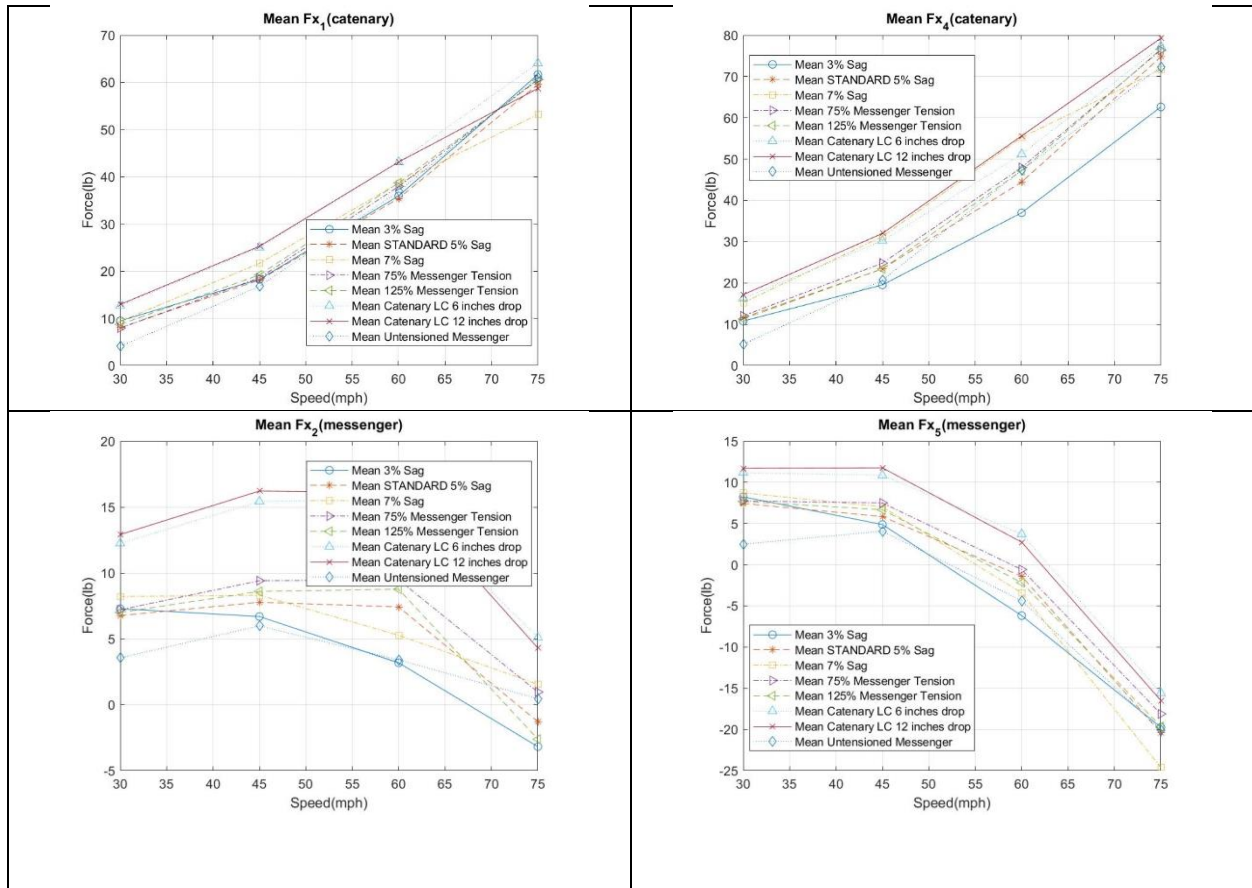


A: 8 - Drag coefficients 45 degrees

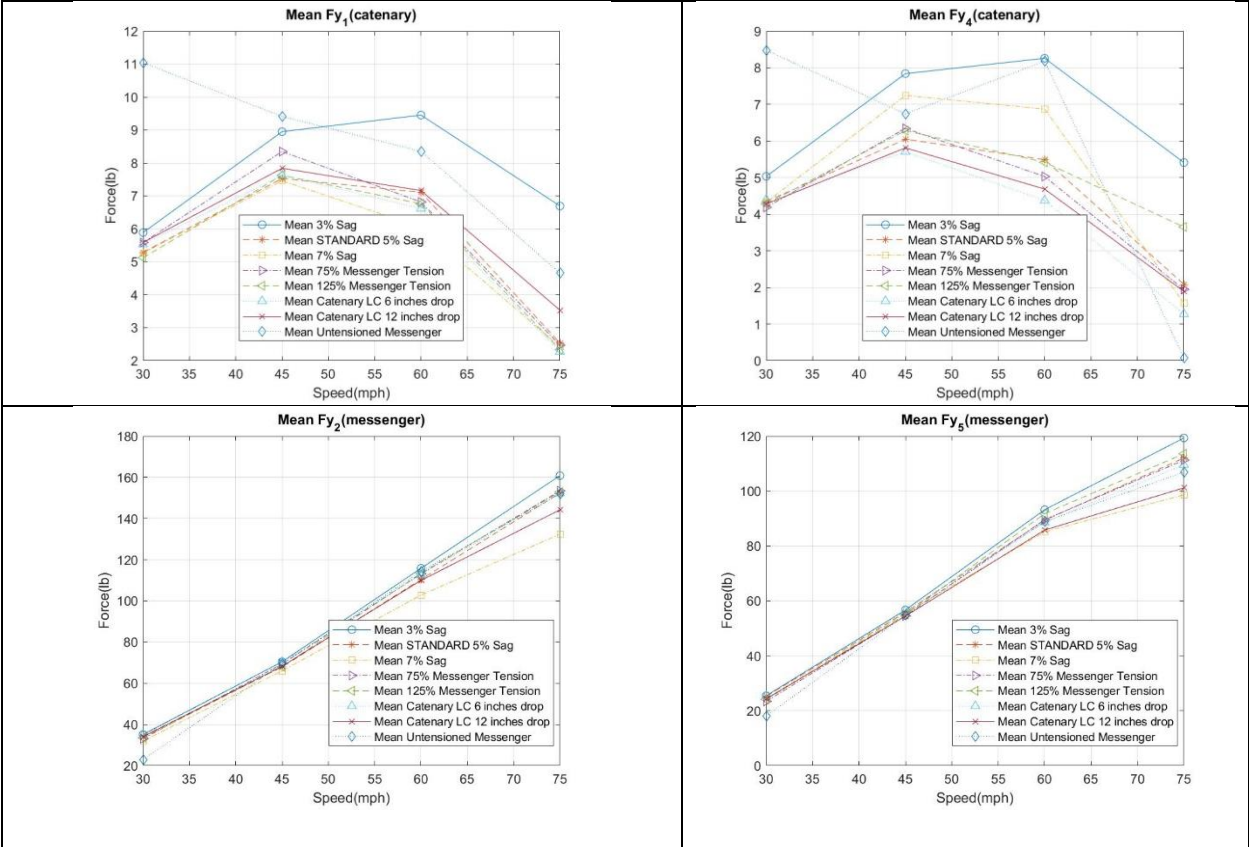


A: 9 - Lift coefficients 45 degrees

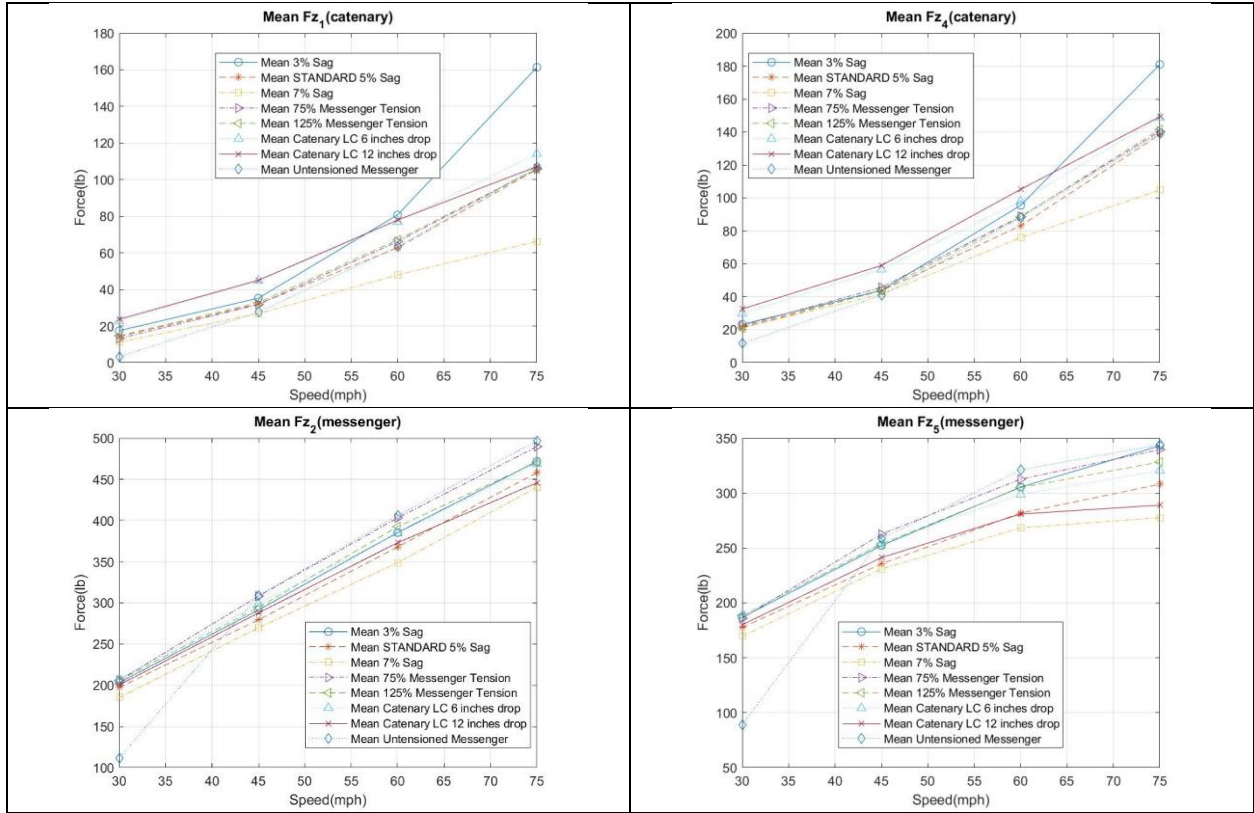
Results for 135 degrees wind angle of attack



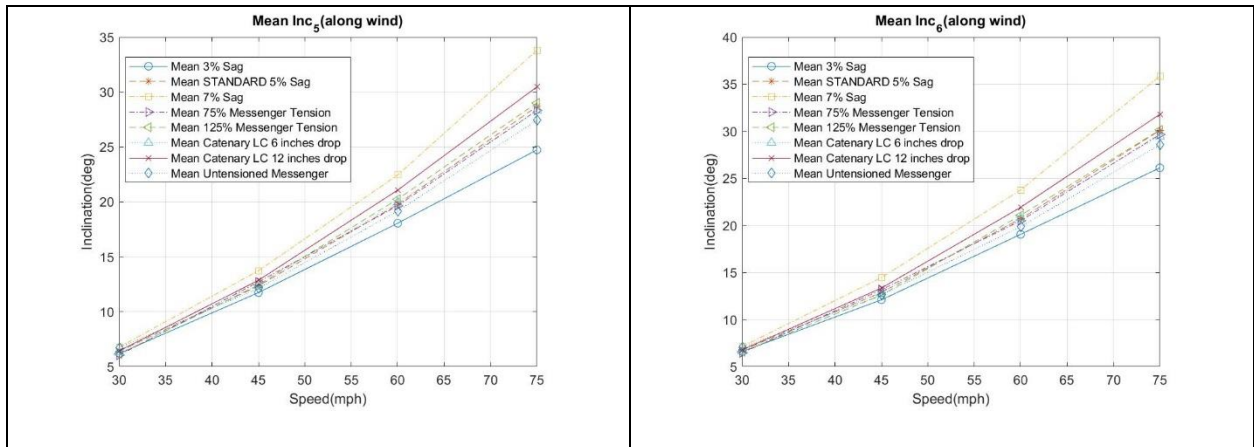
A: 10 - Mean lift forces 135 degrees



A: 11 - Mean drag forces 135 degrees



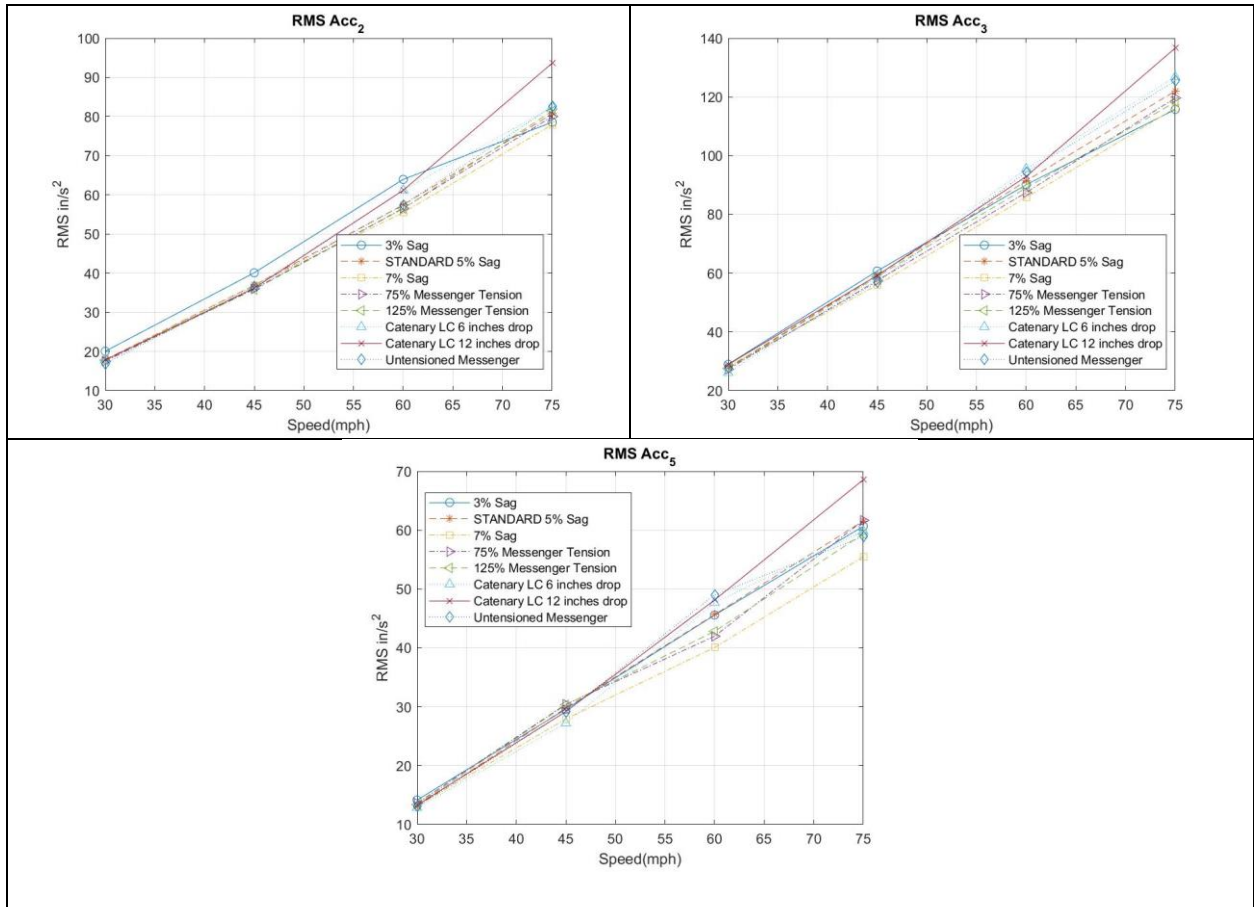
A: 12 - Mean tension forces 45 degrees



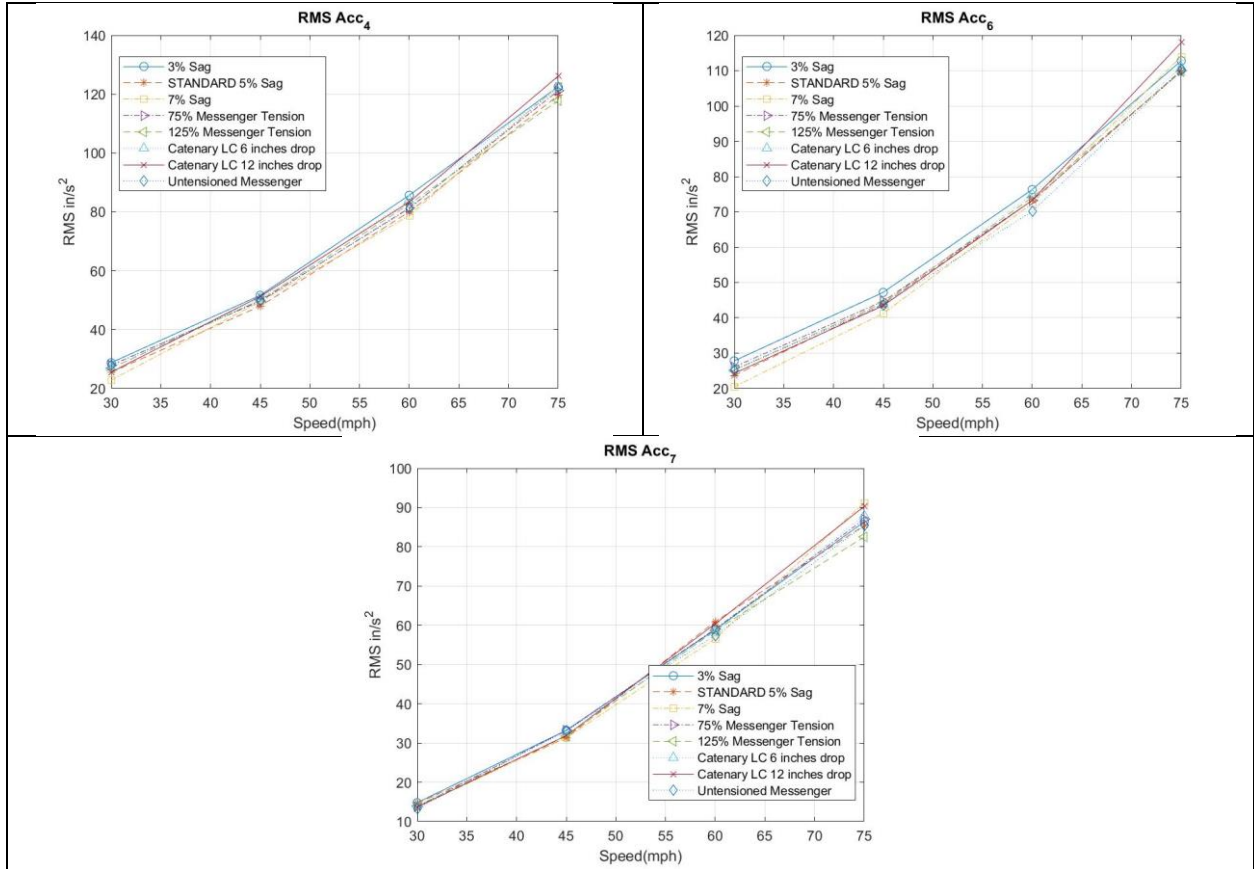
A: 13 - 3-section signal mean inclinations along wind 135 degrees



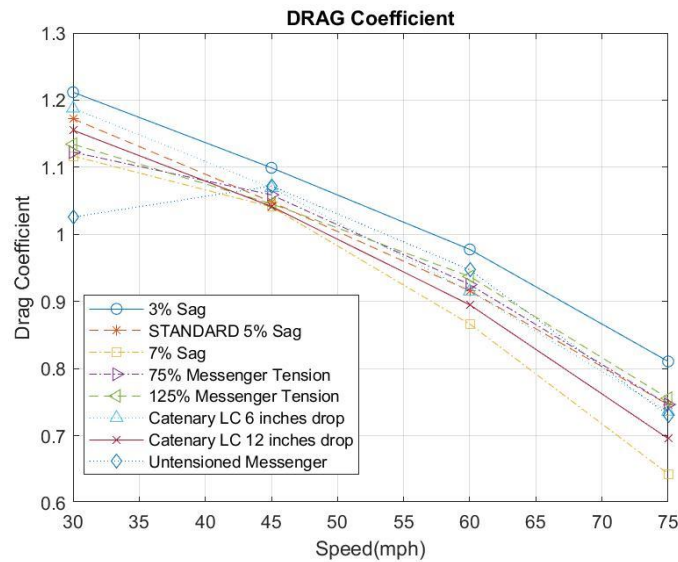
A: 14 - 5-section signal mean inclinations along wind 135 degrees



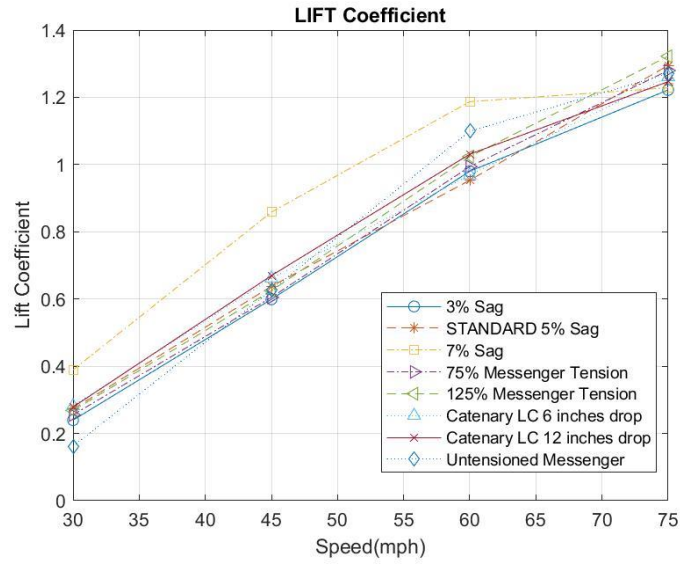
A: 15 - 3-section signal rms of accelerations 135 degrees



A: 16 - 5-section signal rms of accelerations 135 degrees

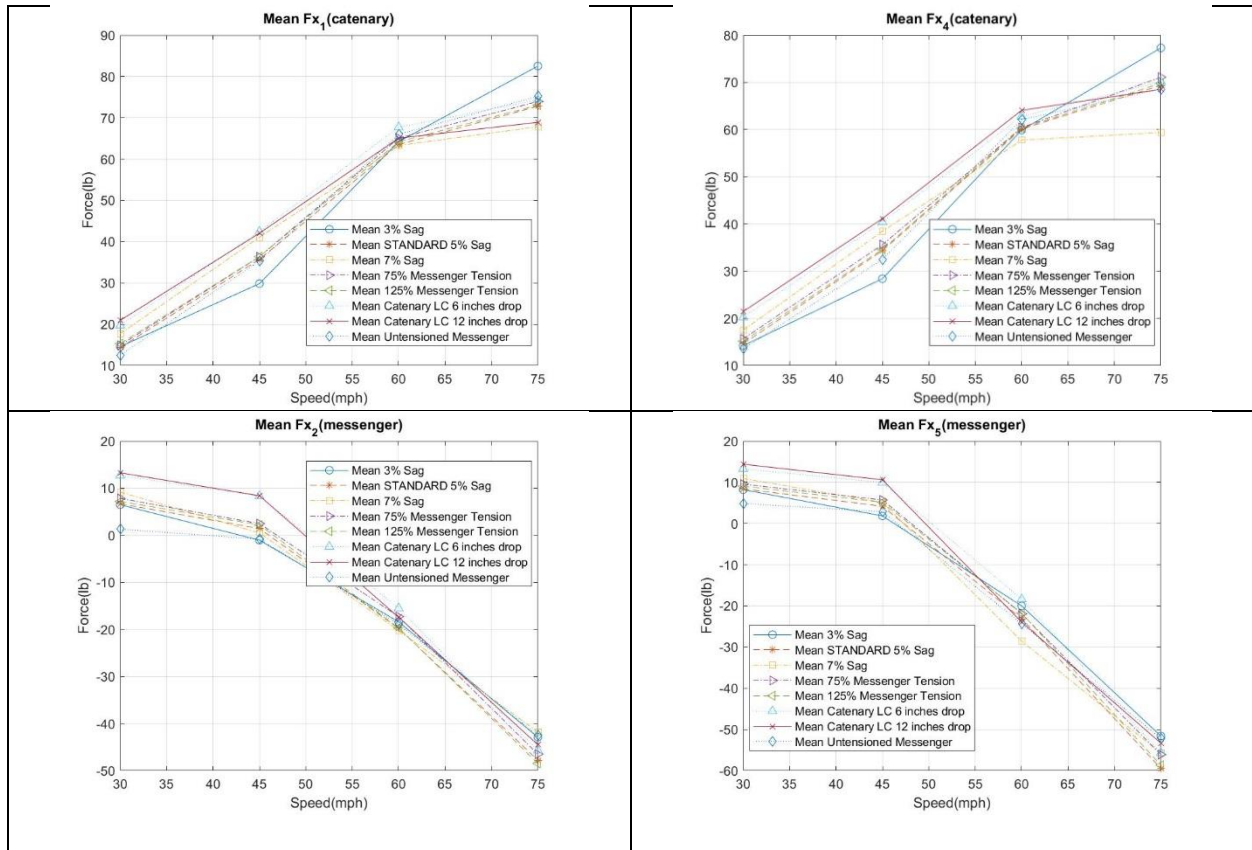


A: 17 - Drag coefficients 135 degrees

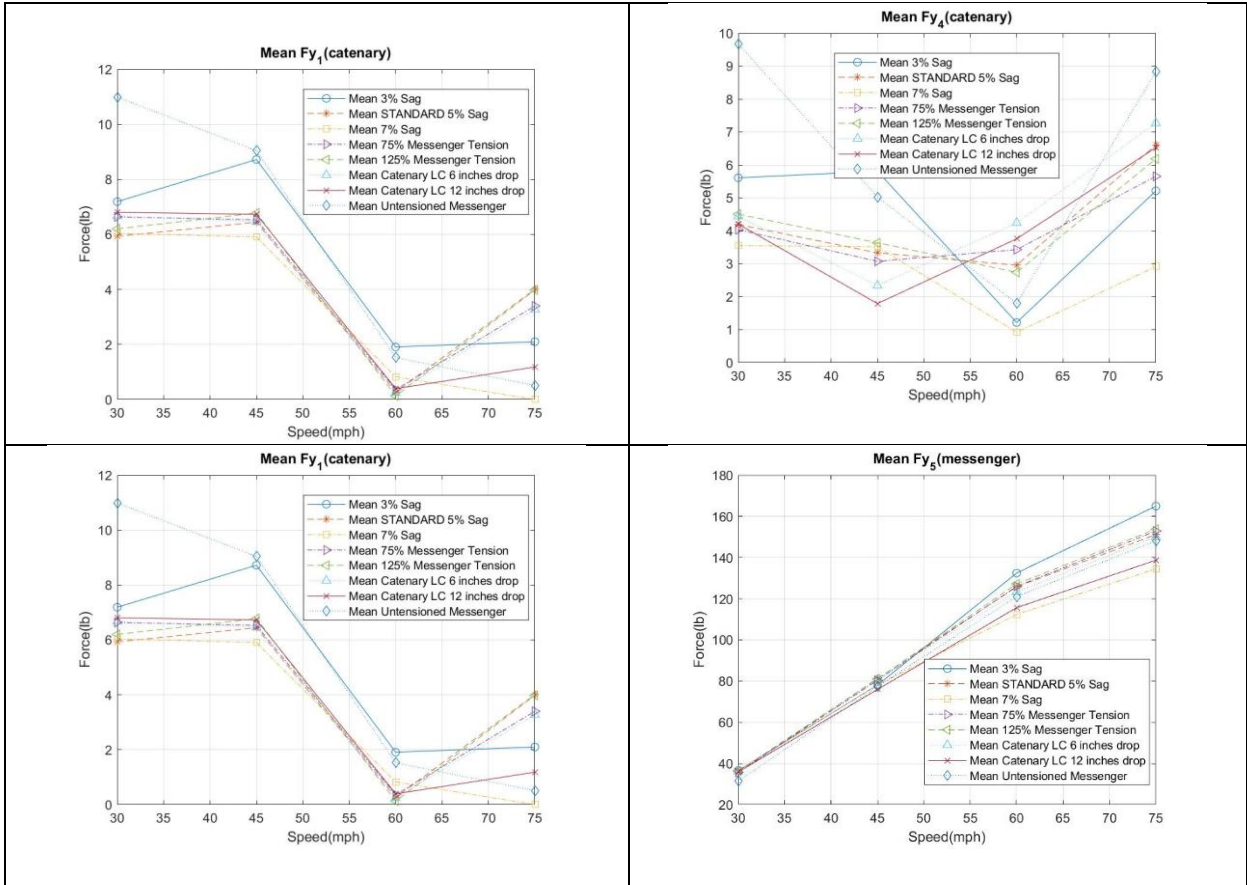


A: 18 - Lift coefficients 135 degrees

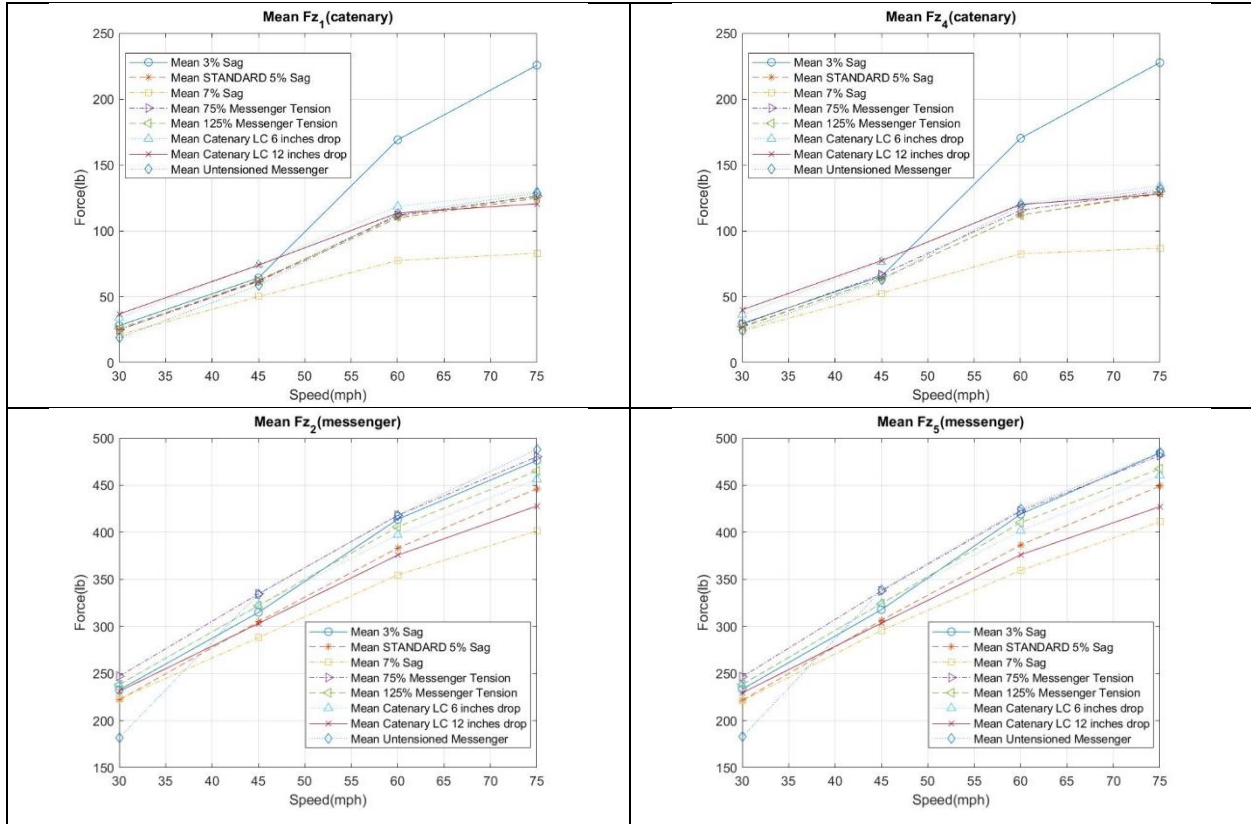
Results for 180 degrees wind angle of attack



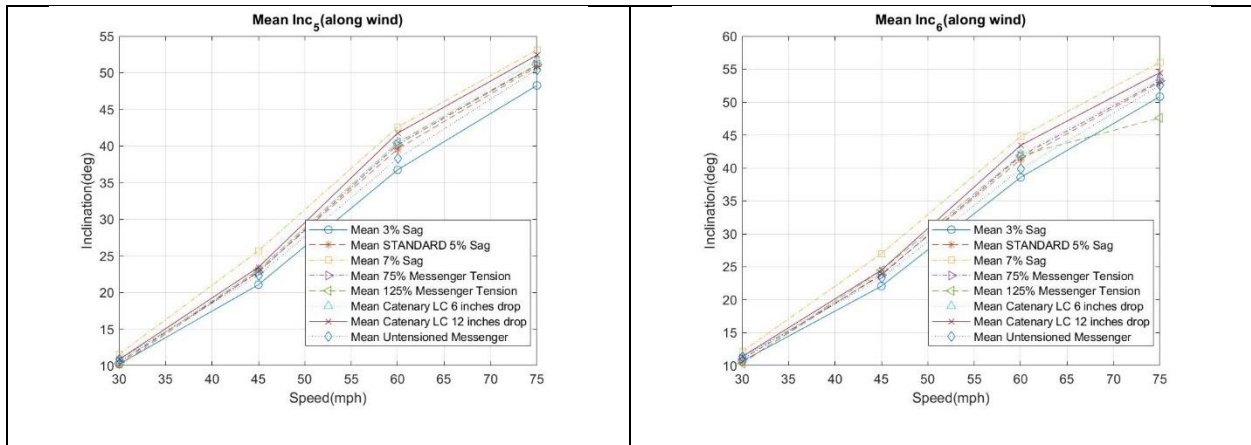
A: 19 - Mean lift forces 180 degrees



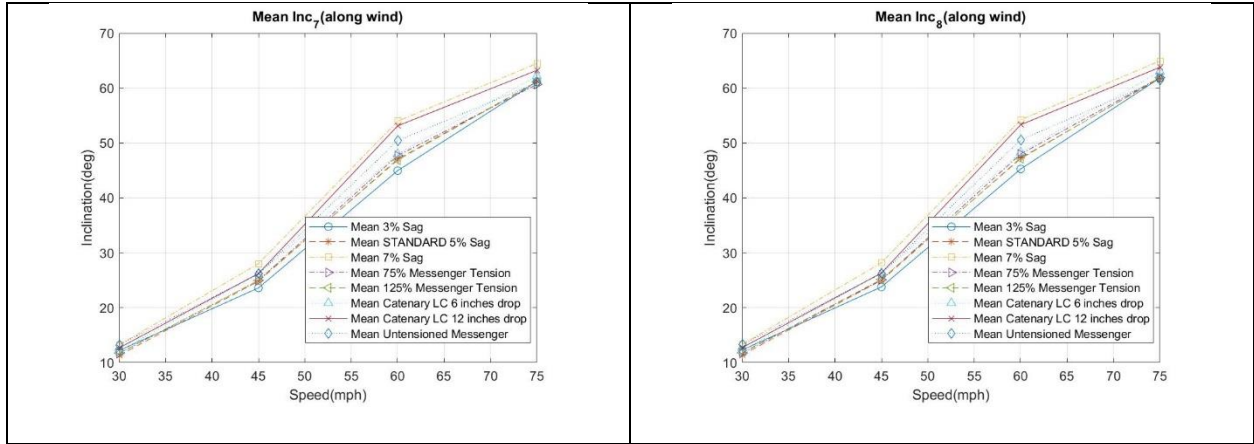
A: 20 - Mean drag forces 180 degrees



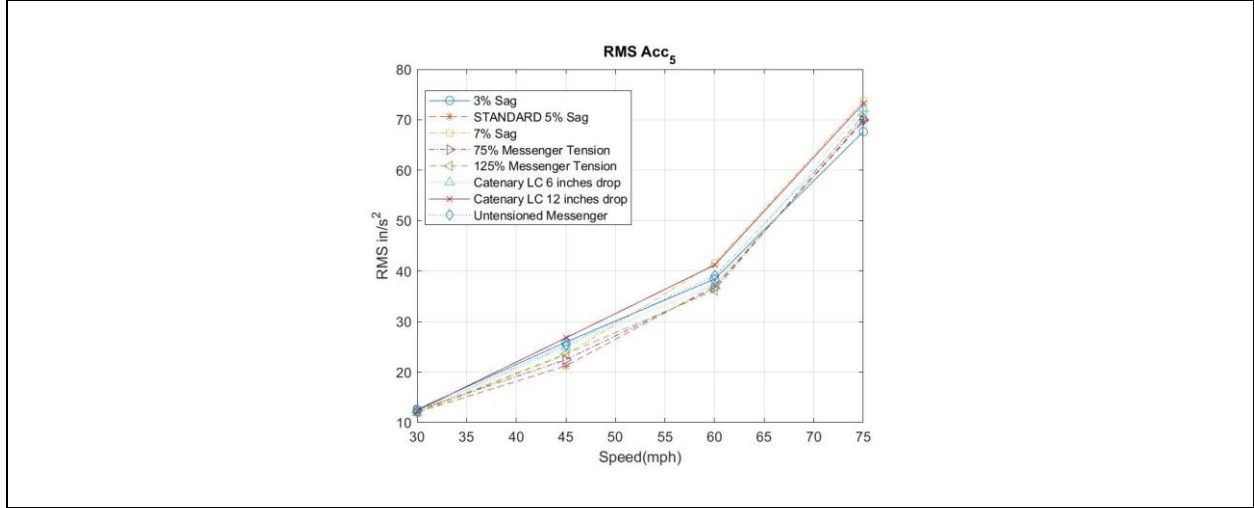
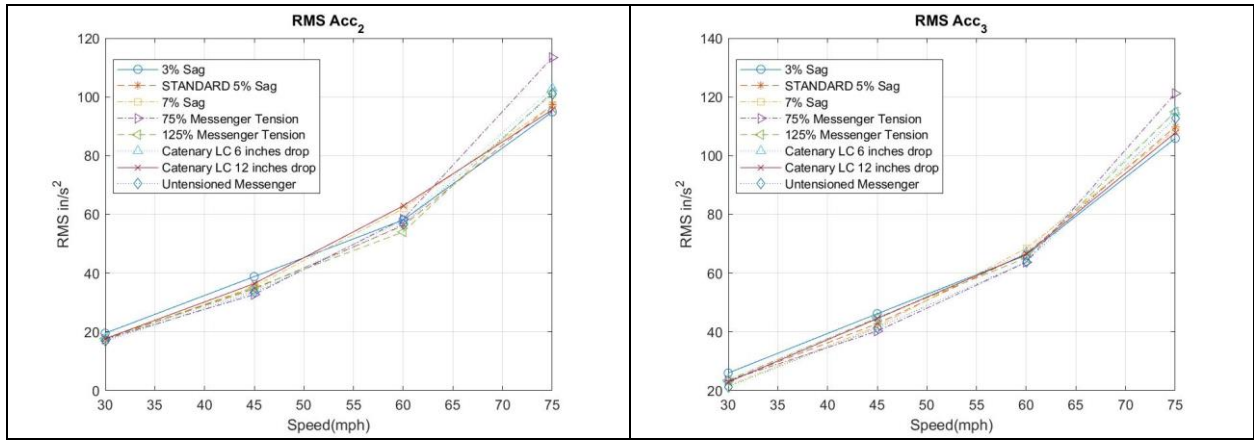
A: 21 - Mean tension forces 45 degrees



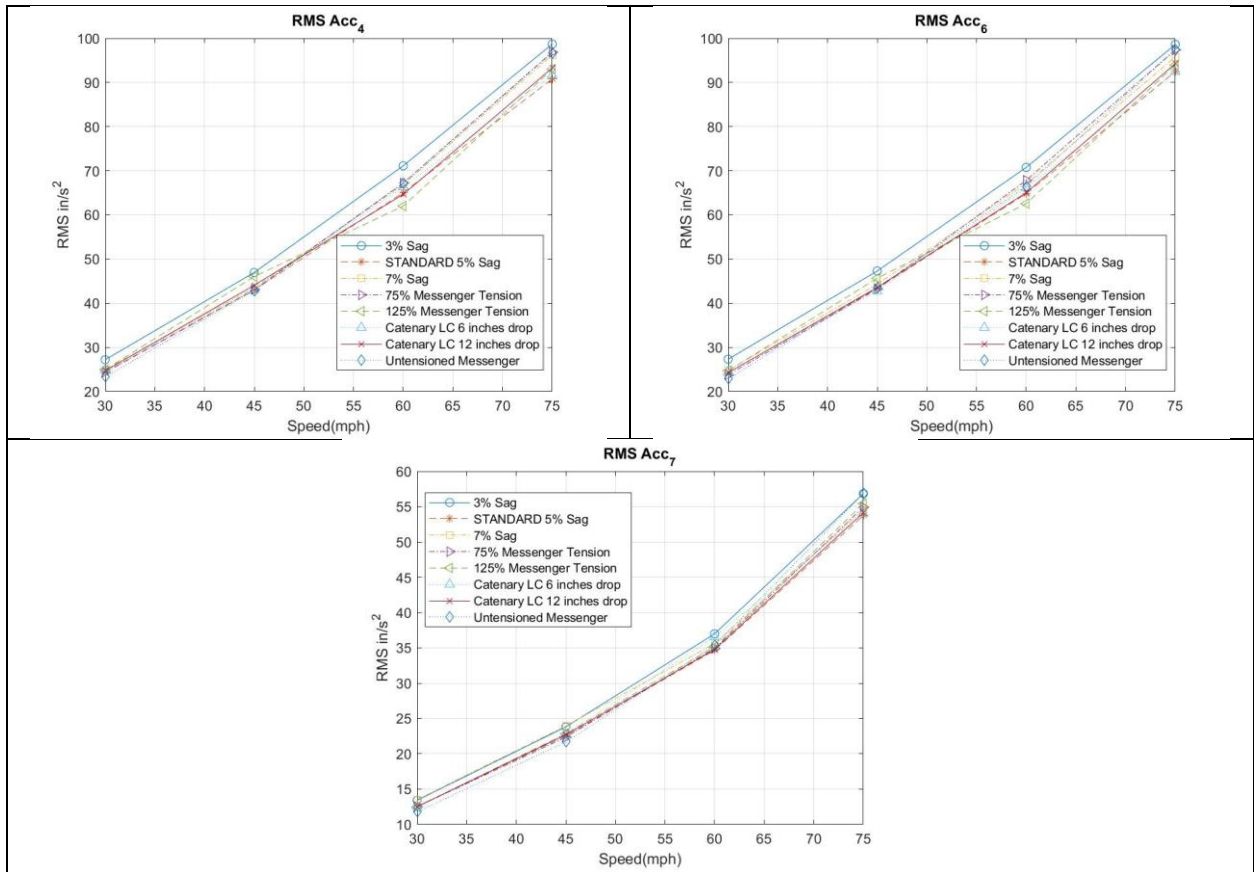
A: 22 - 3-section signal mean inclinations along wind 180 degrees



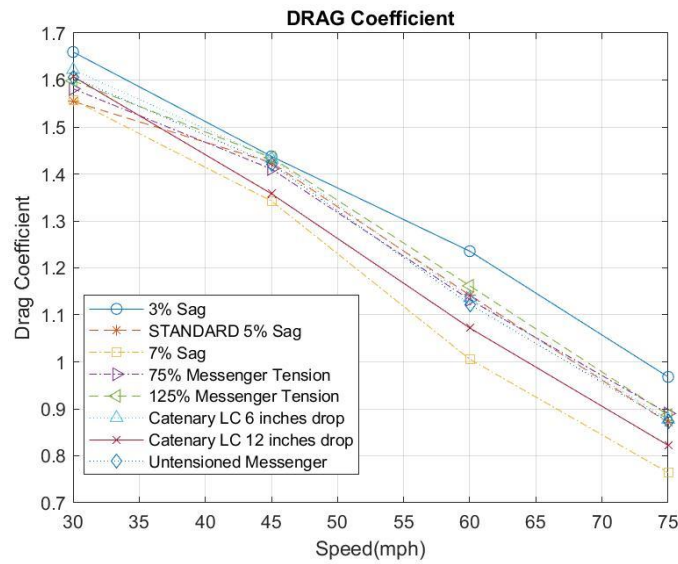
A: 23 - 5-section signal mean inclinations along wind 180 degrees



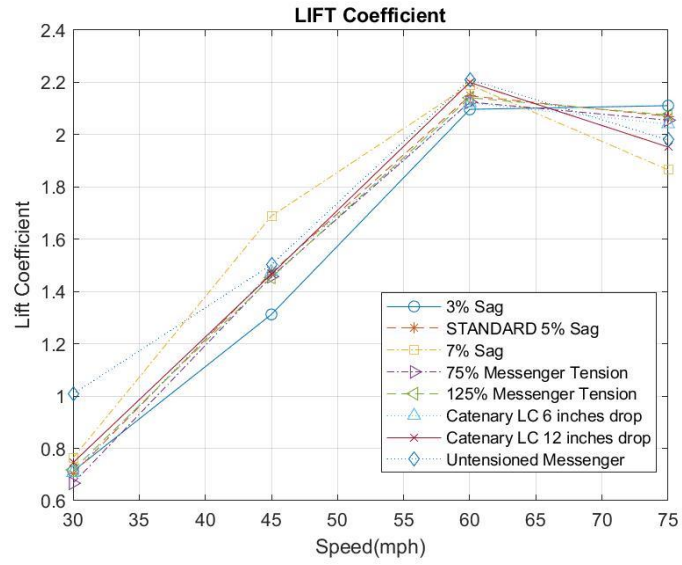
A: 24 - 3-section signal rms of accelerations 180 degrees



A: 25 - 5-section signal rms of accelerations 180 degrees



A: 26 - Drag coefficients 180 degrees



A: 27 - Lift coefficients 180 degrees